Safe-by-design strategies for lowering the genotoxicity and pulmonary inflammation of multiwalled carbon nanotubes: Reduction of length and the introduction of COOH groups

Niels Hadrup, Kristina Bram Knudsen, Marie Carriere, Martine Mayne-L'Hermite, Laure Bobyk, Soline Allard, Frédéric Miserque, Baptiste Pibaleau, Mathieu Pinault, Håkan Wallin, et al.

HAL Id: cea-03284985
https://cea.hal.science/cea-03284985

Submitted on 13 Jul 2021

Journal Pre-proof

Safe-by-design strategies for lowering the genotoxicity and pulmonary inflammation of multiwalled carbon nanotubes: Reduction of length and the introduction of COOH groups

Niels Hadrup (Formal analysis) (Visualization) (Writing - original draft), Kristina Bram Knudsen (Conceptualization) (Investigation) (Writing - review and editing), Marie Carriere (Conceptualization) (Investigation) (Formal analysis) (Visualization) (Writing - original draft), Martine Mayne-L'Hermite (Conceptualization) (Investigation) (Formal analysis) (Visualization) (Writing - original draft), Laure Bobyk (Investigation) (Writing - review and editing), Soline Allard (Conceptualization) (Investigation) (Formal analysis) (Visualization)<ce:contributor-role>Writing - Original draft), Frédéric Miserque (Investigation) (Writing - review and editing), Baptiste Pibaleau (Investigation) (Writing - review and editing), Mathieu Pinault (Investigation) (Writing - review and editing), Håkan Wallin (Conceptualization) (Project administration) (Formal analysis) (Writing - review and editing), Ulla Vogel (Conceptualization) (Project administration) (Formal analysis) (Writing - original draft)

Please cite this article as: Hadrup N, Knudsen KB, Carriere M, Mayne-L'Hermite M, Bobyk L, Allard S, Miserque F, Pibaleau B, Pinault M, Wallin H, Vogel U, Safe-by-design strategies for

lowering the genotoxicity and pulmonary inflammation of multiwalled carbon nanotubes: Reduction of length and the introduction of COOH groups, *Environmental Toxicology and Pharmacology* (2021), doi: https://doi.org/10.1016/j.etap.2021.103702

Safe-by-design strategies for lowering the genotoxicity and pulmonary inflammation of multiwalled carbon nanotubes: Reduction of length and the introduction of COOH groups

Niels Hadrup[a, #], Kristina Bram Knudsen[a, #], Marie Carriere[b], Martine Mayne-L'Hermite[c], Laure Bobyk[b], Soline Allard[c], Frédéric Miserque[d], Baptiste Pibaleau[c], Mathieu Pinault[c], Håkan Wallin[a,e], Ulla Vogel[a,f,*]

[a] *National Research Centre for the Working Environment (NFA), 105 Lersø Parkallé, Copenhagen Ø, Denmark. E-mail addresses: NH: nih@nfa.dk; KBK: bramknudsen@gmail.com; UV: ubv@nrcwe.dk*

[b] *INAC (Institute for Nanoscience and Cryogenics); LAN (Laboratoire Lésions des Acides Nucléiques; Nucleic Acid Lesions Laboratory); 17 avenue des Martyrs 38054 Grenoble cedex 09; France; Email addresses: MC: marie.carriere@cea.fr; LC laure.bobyk@gmail.com*

[c] *Université Paris-Saclay, CEA, CNRS, NIMBE, 91 191 Gif sur Yvette Cedex ; France ; E-mail address MM: martine.mayne@cea.fr; SA: soline.allard@cea.fr; BP: baptiste.pibaleau@gmail.com; MP: mathieu.pinault@cea.fr*

[d] *CEA, DES, Service de la Corrosion et du Comportement des Matériaux dans leur Environnement (SCCME), Laboratoire d'Etude de la Corrosion Aqueuse (LECA), Université Paris-Saclay, F-91191 Gif-sur-Yvette, France ; E-mail address FM: frederic.miserque@cea.fr;*

[e] *National Institute of Occupational Health, Pb 5330 Majorstuen, 0304, Oslo, Norway. E-mail address: HW: Hakan.Wallin@stami.no*

[f] *DTU Food, Danish Technical University (DTU), Anker Engelunds Vej 1, 2800 Kgs. Lyngby DK-2800 Kgs. Lyngby, Denmark*

*Corresponding Author of final publication: Ulla Vogel, National Research Centre for the Working Environment, Lersø Parkallé 105, DK-2100 Copenhagen Ø, Denmark. Telephone: +45 39 16 52 00. E-mail: ubv@nrcwe.dk; *Corresponding author during the submission and review process:* Niels Hadrup, National Research Centre for the Working Environment, Lersø Parkallé 105, DK-2100 Copenhagen Ø, Denmark. Telephone: +45 39 16 52 00. E-mail: nih@nfa.dk.

#N.H. and K.B.K. contributed equally to this publication

HIGHLIGHTS

- We investigated safe-by-design strategies to lower lung toxicity of carbon nanotubes

- Carbon nanotubes were either shortened or had COOH-groups added

- Both strategies lowered pulmonary inflammation measured as neutrophils in lung

- Genotoxicity of long carbon nanotubes was lowered by either strategy

- Overall, the toxicity was lowered, but not eliminated, by either strategy

Abstract

Potentially, the toxicity of multiwalled carbon nanotubes (MWCNTs) can be reduced in a safe-by-design strategy. We investigated if genotoxicity and pulmonary inflammation of MWCNTs from the same batch was lowered by a) reducing length and b) introducing COOH-groups into the structure. Mice were administered: 1) long and pristine MWCNT (CNT-long) (3.9 µm); 2) short and pristine CNT (CNT-short) (1 µm); 3) CNT modified with high ratio COOH-groups (CNT-COOH-high); 4) CNT modified with low ratio COOH-groups (CNT-COOH-low). MWCNTs were dosed by intratracheal instillation at 18 or 54 µg/mouse (~0.9 and 2.7 mg/kg bw). Neutrophils numbers were highest after CNT-long exposure, and both shortening the

2

MWCNT and addition of COOH-groups lowered pulmonary inflammation (day 1 and 28). Likewise, CNT-long induced genotoxicity, which was absent with CNT-short and after introduction of COOH groups. In conclusion, genotoxicity and pulmonary inflammation of MWCNTs were lowered, but not eliminated, by shortening the fibres or introducing COOH-groups.

Article info

3

Introduction

Multi-walled carbon nanotubes (MWCNTs) exhibit extreme material properties with regard to chemical inertness, mechanical strength, thermal and electrical conductivity. Because of these properties, MWCNTs are used in numerous industrial applications, potentially entailing occupational exposure to MWCNTs. Since the physico-chemical properties of multi-walled MWCNTs vary substantially (Jackson et al., 2015), it is important to identify the physico-chemical properties that drive the toxic responses. Previous data have shown that multi-walled MWCNTs are toxic and have a carcinogenic potential (Grosse et al., 2014; Kasai et al., 2016; Knudsen et al., 2018; Nagai et al., 2011; Poulsen et al., 2017, 2016; Rittinghausen et al., 2014; Saleh et al., 2020; Sargent et al., 2014; Suzui et al., 2016; Takagi et al., 2012). Kasai and co-workers demonstrated the carcinogenic potential of one specific multi-walled MWCNT called MWNT-7. This tube was 5.4 to 5.9 µm in length and had a diameter of 93-98 nm. Rats were exposed by inhalation of 0.02, 0.2, or 2 mg/m^3 (6h/day 5days/week for 104 weeks). Lung carcinomas were observed at 0.2 mg/m^3 in male rats (Kasai et al., 2016). MWCNT-7 was classified as possibly carcinogenic to humans by IARC (class 2B) (IARC, 2017).

While MWCNT-7 caused lung cancer by inhalation and several other long and thick MWCNTs caused cancer following intraperitoneal exposure (Rittinghausen et al., 2014), a short and thin MWCNT did not cause cancer after intraperitoneal exposure (Muller et al., 2009). Thus, physico-chemical properties of MWCNTs predict their toxicity, and it may be possible to use this in a safe-by design strategy to reduce the toxicity of MWCNTs. Parameters previously addressed include stiffness, diameter, length, specific surface area and metal contaminations. Catalan and colleagues

4

compared the toxicity of straight and tangled MWCNTs of different sizes in mice. One MWCNT was straight: 4.4 µm in length and 69 nm in diameter, the other was tangled 0.37 µm x 15 nm. The straight MWCNT was given at an inhalation level of 8.2 mg/m^3 (4 h/day for 4 days); it induced genotoxicity as detected in the comet assay – in both bronchoalveolar lavage (BAL) fluid and lung cells. By contrast, after 17.5 mg/m^3 of the tangled, short MWCNT, there were no effects on these endpoints (Catalan et al., 2016).

Concerning studies using intratracheal instillation, we recently showed that total deposited surface area predicted neutrophil influx 1, 28 and 92 days after exposure to 10 different MWCNTs in mice, whereas genotoxicity was predicted by MWCNT diameter (Poulsen et al., 2016). It was recently shown that two different MWCNTs induced inflammation after exposure by inhalation or intratracheal instillation, and that inflammation correlated with the total surface area of the deposited MWCNTs across exposure method 1-3 days after exposure and 28 days after exposure (Gaté et al., 2019). An aspiration study by Catalan and her colleagues, run in parallel to the inhalation study described above, corroborated that long straight MWCNTs were genotoxic and that this was not seen for tangled short MWCNTs (Catalan et al., 2016). Also, with a 3.5 µm long (1-20 nm in diameter) MWCNT (MWCNT-N), Suzui *et al.*, after trans-tracheal intrapulmonary spraying into rat lungs at 3.3 mg/kg bw (1 mg/rat), demonstrated carcinogenicity in the form of malignant mesothelioma and lung tumours (Suzui et al., 2016). After intratracheal instillation, both a long (4.1 µm) and thick, and a short (0.9 µm) and thin MWCNT induced DNA damage in the comet assay (Poulsen et al., 2015b). Notably in one intratracheal instillation study, long MWCNTs (5 µm in length) did not induce genotoxicity in the comet assay (Hadrup et al., 2017).

Modulating the length of MWCNTs may constitute a safe-by-design strategy to

5

reduce the toxicity of MWCNTs; and another strategy is the chemical modification of their surface. Poulsen *et al.* in the 2016 study described above investigated similar tubes modified with –OH, -COOH and NH_2 chemical groups, and found that oxidation via the two former groups were predictors of lower inflammation 28 days after intratracheal instillation into mice (Poulsen et al., 2016). In addition, Hamilton and his colleagues found that carboxylation of MWCNT completely eliminated the bioactive potential of these tubes *in vitro* (Hamilton et al., 2013).

MWCNTs vary with respect to many different physico-chemical properties and often, the treatment required to change one physico-chemical property will introduce additional modifications. This means that often, MWCNTs that are compared, differ with respect to several different physico-chemical properties. In order to be able to make firm conclusions regarding the effect of MWCNT physico-chemical properties on toxicity, we need to compare MWCNTs that only differ for single parameters. In the current work, we set out to test whether shortening MWCNTs or oxidising their surface by adding COOH groups decreased their pulmonary toxicity and genotoxicity. Our H_0 hypothesis was: Shortening or oxidising MWCNTs do not decrease their toxicity; and the corresponding H_1 hypothesis was: Shortening or oxidising MWCNTs decrease MWCNT-induced genotoxicity and pulmonary inflammation. We synthesised one forest of 550 µm long MWCNT. These pristine CNTs were separated into four batches, that received different treatments: dispersion by sonication into two length distributions and oxidation to obtain two different ratio COOH-groups.. Thus, the MWCNTs differed in principle only length and surface oxidation, whereas diameter and thus specific surface area remained comparable (Cohignac et al., 2018; Landry et al., 2016). We tested long (3.9 µm) *vs.* short (1 µm) pristine MWCNT and compared them with ~3 µm long ones modified by addition of COOH-groups. We used intratracheal instillation in

6

mice and after 1, 28 and 90 days determined neutrophil numbers in BAL fluid as a measure of pulmonary inflammation, and a range of other immune cells in BAL fluid. Comet assay was employed to measure genotoxicity in BAL fluid cells, lung and liver cells. In addition, we assessed genotoxicity of the MWCNTs in the A549 human epithelial alveolar cell line, using comet assay, 53BP1 immunostaining and the in vitro cytokinesis-blocked micronucleus assay.

Methods

Nanomaterial synthesis and dispersion

Synthesis of pristine MWCNT batch

MWCNTs were synthesised at CEA-NIMBE in France by aerosol-assisted catalytic chemical vapour deposition (CCVD), which consists in catalytic decomposition of liquid hydrocarbons. Mixed aerosols containing both a liquid hydrocarbon (toluene), as a carbon source, and a metallic precursor (ferrocene), as a catalytic source, were carried in the reactor by an Ar/H_2 gas mixture. Therefore, both carbon and catalytic sources fed simultaneously and continuously the reactor volume (Castro et al., 2013; Charon et al., 2021). The concentration of ferrocene in toluene was 1.25 wt %, the synthesis temperature was 800°C and the duration was 30 min. This process enabled the synthesis of pristine vertically aligned MWCNT exhibiting a length of 550 µm (SEM micrographs on Figure 1 (a)). Such MWCNT contain almost no by-products such as carbon nanoparticles or amorphous carbon (Figure 1b)). They are MWCNTs and their mean diameter measured by TEM is 26 +/- 12,7 nm (Figure 1c) and

7

d)). The residual catalyst content (Fe) was determined by TGA under air and was approximately 2.9 wt %. In our previous studies, it was found that iron is mainly located at the CNT base or inside the CNT core and is enwrapped by graphene layers (Heresanu et al., 2008).

This batch of pristine MWCNT was divided in four parts: two of them were used to make long and short pristine MWCNT dried powder in order to study the effect of their length; the other two were acid treated in order to study the effect of surface oxidation on toxicity. The different procedures involved in this study for the preparation of the different MWCNT batches are based on our previous work (Landry et al., 2016).

Synthesis of CNT-short and CNT-long

MWCNTs were dispersed in toluene without any surfactant, using an ultrasonication probe of 13mm in diameter (Bioblock vibracell 75043) working at 30% of maximum power (750W), in a pulsed mode, 1s/1s. During the sonication, the suspension was maintained at room temperature by using a cooling bath at 0 °C. Sonication time was adjusted to obtain long and short pristine MWCNTs that were well dispersed with no agglomerates. The sonication times were 9h and 70h for 4μm and 1μm long, respectively. The 1μm MWCNTs were fairly straight and the 4μm ones were lightly curved (Depicted in Supplementary Materials Figure S1). Toluene liquid medium was chosen as the liquid medium to individualise MWCNT because the volatility enables easy removal. Thus, dried powders were obtained by heating the suspensions at 60°C under vacuum in order to remove all toluene. Concerning short MWCNT obtained with a long sonication time, titanium pollution (from the sonication probe) was measured and a protocol was established in order to remove all of it by centrifugation (see Supplementary materials, section "purity", Figures S5 and S6). Four

8

suspensions of each MWCNT length were obtained, from which the reproducibility in terms of MWCNT length was confirmed (see Supplementary materials, Figures S2 and S3). The suspensions were well dispersed with individual fairly straight MWCNTs.

Synthesis of CNT-COOH-low and CNT-COOH-high

Part of raw MWCNT underwent acid treatment in order to functionalise MWCNT with COOH groups. As previously, MWCNT were dispersed in toluene without any surfactant using a microprobe of 13mm diameter at 30% of maximum power, in a pulsed mode, 1s/1s, for only 1 h. Then, the suspension was dried by heating under vacuum. The dried powders were then suspended in a mixture of concentrated nitric acid (65%) and sulphuric acid (99%) and refluxed for 20 min at 50°C. High-COOH MWCNT and low-COOH MWCNT batches were obtained with 1:3 and 1:1 in volume ratio (concentrated nitric acid: sulphuric acid) respectively. After washing with deionised water until the supernatant reaches a pH of approximately 7, the samples were dried under vacuum at 60 °C.

Overview of the final MWCNT batches used for toxicity assays

In total, four batches were prepared for the toxicity tests: 1) long and pristine MWCNT (abbreviated CNT-long); 2) short and pristine MWCNT (CNT-short); 3) MWCNT modified with high ratio (in atom) COOH-groups (CNT-COOH-high); 4) MWCNT modified with a low ratio COOH-groups (CNT-COOH-low). The BET surface area of raw MWCNT was measured on selected batches to be 62 m^2/g. The BET surface area of the 4 MWCNTs was assumed to be the same, based on a previous study,

9

showing that BET surface area was unaltered although MWCNT length was modified

(Cohignac et al., 2018; Landry et al., 2016).

Dispersion of MWCNTs for animal experiments

The four batches of MWCNTs were dispersed in 2% serum from sister animals

(C57BL/6JBom mice) in nanopure water. The suspensions (2.56 mg MWCNT/mL)

were made on the day of instillation to avoid re-agglomeration of MWCNTs. They were

sonicated for 16 minutes in a volume of 4 to 6 mL using a 400 W Branson Sonifier S-

450D (Branson Ultrasonics Corp., Danbury, CT, USA mounted with a disruptor horn)

and operated at 10% amplitude and in pulsed mode (10 s on/10 s off) as described in

(Hadrup et al 2017). During this procedure, the dispersions were cooled with ice water

at 0°C. Three-fold dilutions were prepared immediately after sonication and each

dilution was re-sonicated for 2 min. Each dilution was constituted by individual

MWCNTs. The MWCNTs showed fairly straight morphology, with a slight curvature

especially for the longer ones. The morphology was not needle-like (see Figure S1).

Animal study procedures

All procedures complied with the EC Directive 86/609/EEC and Danish law

regulating experiments with animals (The Danish Ministry of Justice, Animal

Experiments Inspectorate permission number 2006/561-1123). C57BL/6J Bom female

mice from Taconic Europe (Ejby, Denmark) (n=246) aged seven to eight weeks

(weighing 19±1 g) were randomised at arrival and housed seven animals per cage.

Female mice were chosen due to their low level of aggression in the cages. The animals

had ad libitum access to tap water or feed (Altromin 1324). Bedding was Enviro Dri,

10

enrichment was hides and play-blocks. Light was on from 6:00 a.m. to 6:00 p.m, the room temperature was 20 ± 2 °C, and the relative humidity $50 \pm 20\%$. The animals were allowed to acclimatise for 7 days before exposure. The animals, now weighing 20 g on average, were administered the MWCNTs by intratracheal instillation under isoflurane anaesthesia as previously described (Hadrup et al., 2017; Jackson et al., 2011; Poulsen et al., 2015b) at 18 or 54 µg/mouse (~0.9 and 2.7 mg/kg bw) at a dose volume of 50 µl (0.36, and 1.08 mg/mL). The doses were chosen based on previous studies (Halappanavar et al., 2019; Jagiello et al., 2021; Knudsen et al., 2018; Poulsen et al., 2013, 2017, 2016, 2015a, 2015b). N was 7 mice per treatment group. Three control mice were instilled with vehicle on each nanomaterial dosage day; in total, this adds up to 12 vehicle controls. However, this study on 4 MWCNTs was part of a larger animal study, including other particles not reported here; thus the total number of controls was n=45 (1 day of recovery), n=30 (28 days) and n=31 (90 days); these controls were all included in the statistical analyses. Recovery periods were 1, 28 and 90 days. The animals were monitored every day. At the end of study, the animals were humanely killed by ZRF anaesthesia (Zoletil Forte 250 mg, Rompun 20 mg/mL, Fentanyl 50 µg/mL in isotonic saltwater) administered intramuscularly at 0.4 mL/100 g bw followed by withdrawal of a large volume of blood directly from the heart using an injection needle. The blood (500-800 µL) was collected in 1.5 mL Eppendorf tubes with K_2-EDTA, plasma was produced by centrifugation and stored at -80°C until analyses. Lung and liver samples for comet assay were snap-frozen in liquid nitrogen, and stored at -80°C until analyses.

11

BAL fluid recovery and cellularity

Inflammation was assessed in terms of cells in BAL fluid as described (Kyjovska 2015). In brief, BAL fluid was recovered by flushing the lungs twice each with 1 mL saline /25 g bw. The samples were centrifuged at 400 x g at 4°C for 10 min; recovered cells were re-suspended in 100 µL HAM-F12 medium (Prod no. 21765037, Invitrogen, Carlsbad, CA, USA) added 10% foetal bovine serum (Prod no. 10106169, Invitrogen, Carlsbad, CA, USA). To determine the cellularity, 40 µL of the resuspension was collected on microscope slides by centrifugation at 60 x g for 4 min in a Cytofuge 2 (StatSpin, Bie and Berntsen, Rødovre, Denmark). Next, cells were fixed using 96% ethanol and stained with May-Grünwald-Giemsa stain. The total cell number was determined with a NucleoCounter NC-100 (Chemometec, Allerød, Denmark) Live/Dead Assay. Differential cell counting was done on 200 cells per sample. For comet assay analysis, 160 µL of 90% HAMF12, 10% FBS, 1% Dimethyl sulfoxide was added to 40µl of the BAL fluid cell suspension.

Levels of DNA strand breaks in the in vivo study

DNA strand breaks were determined in BAL fluid cells, lung and liver tissue using the comet assay as described (Jackson et al., 2013). The percentage of DNA in the tail was measured by comet assay using the IMSTAR PathfinderTM apparatus (Jackson et al., 2013). In brief, BAL fluid cells were thawed at 37˚C. Pieces of frozen lung and liver were homogenised directly in Merchant's medium (140 mM NaCl 1.5 mM KH_2PO4, 2.7 mM KCl, 8.1 mM Na_2HPO_4, 10 mM Na_2-EDTA, pH 7.4) using a steel mesh mounted in a syringe. The isolated cells were then incubated overnight in lysis buffer at 4˚C. The slides were then rinsed in electrophoresis buffer (pH >13) and subjected to 40 min of alkaline treatment. Electrophoresis was run for 25 min at a

12

current of 300 mA and an applied voltage of 1.15 V/cm. Next, the slides were pH

neutralised, fixed in 96% ethanol and left on a 45˚C heating plate for 15 min. The cells

were added SYBR®Green fluorescent stain, a UV-filter, and cover slips. After analysis

in the IMSTAR PathfinderTM system, the average value of percentage tail DNA was

calculated for all cells scored in each Trevigen CometSlide well. Negative and positive

controls were included on all slides, and were non-exposed A549 cells, and A549 cells

exposed to 30 µM H_2O_2, respectively. Each data point was normalised to the negative

controls on each slide to adjust for day-to-day variation.

For quantification of 8-oxo-dG by HPLC-tandem mass spectrometry (HPLC-

MS/MS), DNA from lungs was extracted and digested as described by Ravanat et al.

(Ravanat, 2002). 700 µL of lysis buffer A (320 mM sucrose, 5 mM $MgCl_2$, 10 mM Tris,

0.1 mM deferroxamine, 1% triton X-100, pH 7.5) was added to half lung and grinded

using a TissueLyzer (Qiagen). After centrifugation for 5 min at 1500 x g, the pellet was

homogenised in 700 µL of lysis buffer B (5 mM EDTA, 10 mM Tris, 0.15 mM

deferroxamine), to which 10% SDS was added. After treatment with RNase A, RNase

T1 and protease, the DNA was precipitated in sodium iodide (NaI)/isopropanol, then

washed with ethanol, and suspended in 0.1 mM deferroxamine. DNA was then digested

to nucleosides first by incubation with nuclease P1, DNase II and phosphodiesterase II

at pH 6 (2 h). In a second step, it was digested with alkaline phosphatase and

phosphodiesterase I (2 h, pH 8). The solution was neutralised with 0.1 µM HCl and

centrifuged. The supernatant was collected, filtered on 0.22 µm filter units, and injected

onto the HPLC-MS/MS system. The API 3000 mass spectrometer (SCIEX) was used in

the multiple reaction monitoring mode with positive electrospray ionisation. The

monitored fragmentation was m/z 284 [M + H]+ → m/z 168 [M + H -116]+ for 8-oxo-

dG. Chromatographic separations were achieved using a C18 reversed phase Uptisphere

13

ODB column (Interchim, Montluçon, France). The elution was performed using a gradient of methanol in 2 mM ammonium formate at a flow rate of 0.2 mL.min-1. The retention time was around 29 min. In addition to the MS spectrometer, the HPLC eluent was analysed in a UV detector set at 270 nm to quantify the amount of unmodified nucleosides. Levels of 8-oxo-dG were expressed as number of lesions per million of normal bases.

In vitro study

The in vitro study was performed on A549 human lung epithelial alveolar cells (ATCC CCL-185), grown in DMEM medium (4.5 g/L glucose) containing 10% fetal bovine serum (FBS), 1% non-essential amino acid (NEAA) and 1% penicillin/streptomycin. Cells were seeded in the appropriate dish, i.e., 6 well-, 12-well, -96 well plates or 58 cm² Petri dishes so that they reached 90% of confluence at the end of exposure time. MWCNTs were pre-wetted in 96% ultrapure ethanol, then diluted in 0.05% w/v sterile-filtered BSA and sonicated twice for 2 min, in pulsed mode (1s on/1s off), using a Vibra Cell 75043 ultrasonicator (Bioblock scientific) operated at 28% amplitude, i.e. 16.7 W (Brun et al., 2014). During the sonication, the MWCNT suspension was cooled in a water-ice bath. Then, the MWCNTs were diluted in FBS-free cell culture medium and applied to cells at 1-100 µg/mL for cytotoxicity evaluation and 50 µg/mL for all other experiments. MWCNT cytotoxicity was evaluated via the WST-1 assay (Roche Diagnostics, Mannheim, Germany), after 24 h of exposure to MWCNT. At the end of the exposure period, the exposure medium was replaced by 100 µl of WST-1 solution, which was incubated for 1h at 37°C. Then, in order to avoid any optical interference from MWCNT remaining adsorbed on cell membranes, plates were centrifuged for 5 min at 200 rcf and 50 µL of supernatant from each well was

14

transferred to a clean 96-well plate. WST1 cleavage by live cells was evaluated by absorbance measurement at 450 nm and corrected from background absorbance, measured at 650 nm.

Genotoxicity was assessed using the comet assay, micronucleus assay and 53BP1 immunostaining. The comet assay was used to evaluate the presence of strand breaks and alkali-labile sites in DNA (alkaline version), as well as Fpg-sensitive (formamidopyridine DNA glycosylase-sensitive) sites and among them 8-oxo-dG (Fpg-modified version). Cells were exposed to MWCNTs in 12-well plates and after 24 h of exposure, they were collected and frozen in storage buffer (85.5 g/L sucrose, 50 mL/L DMSO, prepared in citrate buffer (11.8 g/L), pH 7.6); they were stored at -80°C until analysis. Ten thousand cells were mixed with 0.6% low melting point agarose and deposited on a slide that had been previously coated with agarose (n=6). After solidification of agarose for 10 min on ice, the slides were immersed in cold lysis solution (2.5 M NaCl, 100 mM EDTA, 10 mM Tris, 10% DMSO, 1% Triton X-100, pH10) overnight at 4°C, then rinsed in 0.4 M Tris pH 7.4. Then, 3 slides were treated with 100 μL Fpg (5 U/slide) for 45 min at 37 °C; the 3 other ones were treated only with Fpg buffer. DNA was allowed to unwind for 30 min in alkaline electrophoresis solution (300 mM NaOH, 1 mM EDTA, pH > 13), then slides were exposed to an electric field of 24 V (300 mA) for 30 min. Slides were then neutralised in 0.4 M Tris pH 7.4 and stained with GelRedTM (Biotium). As positive control for alkaline comet assay, 50 µM H_2O_2 was directly deposited onto control slides (unexposed cells), then incubated for 5 min at room temperature. As positive control for comet-Fpg, A549 cells were exposed for 20 min at 37 °C to 1 µM riboflavin, then to 10 J/cm² of UVA. At least 50 comets per slide were analysed using Comet IV software (Perceptive Instruments, Suffolk, UK);

15

results are expressed as % tail DNA (n=3). The absence of MWCNT aggregates in comets, which would potentially interfere with DNA migration, was visually verified.

In order to investigate chromosomal damage, the cytokinesis-blocked micronucleus assay was performed as described by Fenech et al. (Fenech, 2000). Cells were seeded in black 96-well plates with transparent bottom, and exposed for MWCNT for 24 h. After exposure, the exposure medium was discarded and cells were cultured for another 24 h in complete cell culture medium containing 4 µg/mL of cytochalasine B that blocks cytokinesis. Cells were then fixed for 15 min in 4% paraformaldehyde and stained with DAPI (15 min, 10 µg/mL) and phalloidin-FITC (200 nM, 30 min). As positive control, A549 cells were exposed for 24 h to 50 ng/mL mitomycin C. Then using a high throughput screening/high content analysis (HTS/HCA) automated microscope (CellInsight CX5, ThermoFisher Scientific), the presence of micronuclei was searched for in 3000 cells per well (with at least 1000 binucleated cells), using 5 independent replicates (5 wells) per condition. Visual inspection ensured that no large MWCNT aggregates interfered with the automatic detection of micronuclei.

To assess the presence of double strand breaks, and by extension the presence of oxidative damage to DNA, foci of 53BP1 DNA repair protein were labelled (Rothkamm et al., 2015) and automatically counted using a CellInsight CX5 high content screening platform (ThermoFisher Scientific). Cells were seeded in black 96-well plates with transparent bottom, then exposed for 24 h to MWCNT. They were then fixed for 20 min with 4% paraformaldehyde, and incubated with as anti-53BP1 antibody (Acris, dilution 1/1500, vol./vol., 1 h at room temperature), then with an anti-rabbit secondary antibody coupled to Atto488 (1/2000, vol./vol., 1 h at room temperature). As positive control, cells were exposed to 10 µM of etoposide for 24 h. Cell nuclei were stained for 15 min with DAPI (1 µg/mL). Total number of 53BP1 foci was

16

automatically counted in 200-400 cells per well (5 wells per exposure condition).

Again, visual inspection ensured that no large MWCNT aggregates interfered with the

automatic detection of 53BP1 foci.

Determination of ROS Generating Ability in cell-free environment

For determination of the effects of MWCNTs on ROS determinations in cell free

media, 2′, 7′-Dichlorofluorescein diacetate (DCFH-DA) was chemically hydrolysed to

dichlorodihydrofluorescin (DCFH) in alkaline solution as described in (LeBel et al.,

1992). DCFH can be oxidized to fluorescent 2′, 7′-dichlorofluorescein (DCF) by

hydroxyl radicals, peroxynitrite, and nitric oxide (LeBel et al., 1992; Rota et al., 1999).

Eleven mg of dry autoclaved MWCNT was sonicated three times of each 8 min on ice-

bath. Two millilitres of saline solution was added before each sonication round. The

sonicator (Branson Sonifier S-450D, Branson Ultrasonics, Danbury, CT) was equipped

with a disruptor horn (model no.: 101-147-037). Each sonication round was done at

10% amplitude with alternating pulses of 10 sec on and pauses of 5 sec. The sonicated

suspensions were diluted to 1, 2, 4, 8, 17, 34, 68 and 100 µg/mL. A control with no

MWCNTs was also prepared. The dilutions were sonicated for an additional 2 min and

incubated with MWCNTs in 3 replicates for 3 hours. Carbon black Printex 90 was

included as a benchmark particle. DCF was measured at kex 5 490 and kem 5 520 nm

on a spectrophotometer (Victor Wallac-2 1420, Perkin Elmer, Denmark). Positive

controls were H_2O_2 and horseradish peroxidase, and the results presented as H_2O_2

equivalents as described previously (Jacobsen et al., 2008).

17

Statistical analyses

Statistical calculations were done in the Graph Pad Prism 7.02 software package (Graph Pad Software Inc., La Jolla, CA, USA). First, each data set was tested for normality with the Shapiro-Wilk test. The ANOVA test is robust against deviations in normality and was used for inter-group comparisons, except when the *p*-value of the Shapiro Wilks test was very low ($p<0.001$); or when the standard deviations of the groups were determined to be highly different. Differences in standard deviations were assessed using the Brown-Forsythe test for three or more treatment groups ($p<0.001$). The latter test was applied because the ANOVA test is somewhat sensitive to differences in data variability. In case of deviations in normality or in inter-group standard deviations, the non-parametric Kruskall-Wallis test was calculated. In order to assess inter-group differences in one-way ANOVA or the Kruskall-Wallis test, multiple comparisons post tests were applied. These were Holm-Sidak's multiple comparisons test (ANOVA) or Dunn's multiple comparisons test (Kruskall-Wallis test). Each MWCNT type was tested independently against the vehicle-control. In order to test across each material each dose level of CNT-short, CNT-COOH-high, and CNT-COOH-low were tested against the respective dose levels of CNT-long using Bonferroni-corrected (6 comparisons) *p*-values for in vivo studies, and 3 comparisons for in vitro studies. Linear regression analysis was done on neutrophil numbers in BAL fluid as function of MWCNT length and oxidation. Scatter plots of the data were reviewed to ensure that the data roughly fitted a line. Next linear regression was calculated, including whether the slope was significantly non-zero. Control values were not included in the linear regression analyses, as a control value does not represent any length nor any O/C ratio.

18

Results

Physical-chemical characterisation of MWCNTs

Length distribution: Table 1 shows the mean lengths of the four batches used for the biological studies. These batches were obtained after a first step involving sonication and acid treatment followed by a subsequent step, which involved dispersion in the biological medium. The latter dispersion using very gentle conditions in comparison to the conditions used for the first step (details provided in the Methods section). The second step ensured re-dispersion of the MWCNTs in biological medium without significant modification of their length. The MWCNT length distribution in the four batches used for biological studies is summarised in Table 1, and illustrated in the Supplementary materials Figure S2. It is noteworthy that the two functionalised MWCNT batches have similar mean lengths, which are comparable to the one of CNT-long. The CNT-short is approximatively four fold shorter than CNT-long.

Surface chemical analysis: The surface chemical analysis was performed through XPS measurements as described in the Supplementary materials. The XPS survey spectra obtained for CNT-COOH-high and low are presented and compared to CNT-long in Figure 2. These three MWCNTs have a different surface chemical composition while having comparable mean length, diameter and specific surface area. The survey spectrum of Figure 2 highlights the main peaks indicating the occurrence of mainly C and O. The binding energy of the main carbon core level (C-1s) exhibits a major contribution of sp^2 carbon, similar whatever the sample, indicating that the carbon structure is still mainly composed of sp^2 carbon, and is not significantly changed by functionalisation treatments. Therefore, the acid treatment has not damaged the integrity of MWCNT structure. However, it is important to note that the intensity of

19

oxygen (O-1s) peak increased with the duration of acid treatment (see magnification of the O-1s peak).

Figure 3 shows the magnification of the C-1s spectrum with the attribution of the different peak chemical contributions. The reference binding energy of the different contributions for the C-1s spectrum are detailed in Table 2. Apart from the Csp^2 and Csp^3 contributions in the C1s peak, carbon is bonded to oxygen according two configurations: C=O at 288.8 eV and C-O at 286.7 eV. The first one is related to COOH groups, and the second one is related to C-OH groups originated from an alcohol or a carboxyl environment. Figure 3 shows that COOH peak intensity increases when acid treatment duration increases. Such results demonstrate that the functionalisation process was effective and that the surface of functionalised MWCNT is partially constituted of COOH and COH bonds.

Concerning the amount of O incorporated at the MWCNT surface, the overall O/C ratio was calculated from the O-1s and the C-1s area ratio. Table 1 presents the average values of the O/C ratio obtained after acid treatment. The results indicate that the proportion of O is significantly higher in functionalised MWCNT as compared to raw long MWCNT. In addition, the proportion of oxygen is about two fold higher in CNT-COOH-high as compared to CNT-COOH-low.

Structure: Raman spectroscopy measurements were performed to analyse the carbon structure. In multi-walled carbon nanotubes, Raman spectrum exhibits D and G bands. The D band is associated with defects and disorder, while the G band is inherent to in plane tangential stretching of carbon-carbon bonds. The ratio between the D and G band intensities (I_D/I_G) is commonly used as a qualitative measurement of the defect density in defective tubes: the higher this ratio, the lower the crystalline level (Charon et al., 2021; Maultzsch et al., 2002; Pimenta et al., 2007). Table 1 reports the

20

ID/IG ratio of the different samples. The spectra obtained for CNT-COOH-low and high are presented in the supplementary information.

As the ratio ID/IG is equivalent to CNT-long one (Table 1), the overall MWCNT surface structure is preserved for the CNT-COOH-low sample even if a low oxygen content is added through the acid treatment (shown by XPS). When the acid treatment is stronger (CNT-COOH-high sample), the ID/IG ratio increases, indicating that the MWCNT structure is affected by acid treatment. This result suggests structural modifications at the MWCNT surface corresponding to COOH grafting, especially for strong acid treatment, which is in agreement with the XPS data showing the occurrence of O bonded to C atoms.

Summary of the physical chemical characterisation: All characteristics of the different batches are summarised in Table 1. Since the sp^2 structure appeared to be preserved whatever the shortening or acid treatment, and according to the different TEM observations we carried out, diameter is not significantly changed by the subsequent procedures. Therefore, the diameter distribution of the different batches involved in this study (long, short, low and high COOH) is similar to that of the raw MWCNT ca. 26.0 ± 12.7 nm (Figure 1). For the animal study, the MWCNTs were dispersed in 2% sibling serum in water as previously described (Hadrup et al., 2017; Knudsen et al., 2018; Poulsen et al., 2016, 2015b).

Body weight

The body weight was not different among the treatment groups throughout the study (data not shown).

Inflammation response

On day 1, CNT-long increased the neutrophil number at both 18 and 54 µg/mouse (Figure 4). For CNT-short and CNT-COOH-high, neutrophils were only increased at the highest dose; CNT-COOH-low exhibited a similar pattern as the former two fibres, although the lowest dose was statistically significantly different from control (Figure 1). When testing across materials, the lowest doses of all three modified materials CNT-short, CNT-COOH-high, and CNT-COOH-low induced lower neutrophil numbers than CNT-long (Figure 4). Macrophage numbers (day 1) were decreased in all treatment groups except for CNT-short (both doses) (Supplementary Table S1). Eosinophils (day 1) were increased in all treatment groups; lymphocytes (day 1) were increased only for CNT-COOH-low (both doses). Total cells on day 1 exhibited a pattern similar to neutrophils and eosinophils (all data are presented in tabulated form in the Supplementary materials Table S1).

On day 28, CNT-long and CNT-COOH-low induced neutrophil influx in BAL fluid at both doses; CNT-COOH-high induced inflammation at the highest dose, whereas CNT-short had no effect (Figure 5). When testing across materials CNT-short high dose induced less inflammation than CNT-long (Figure 5). The major effect on macrophages (day 28) was increased in this cell type at the highest dose of CNT-long. Eosinophil (day 28) cell numbers were increased at both doses of CNT-long. Lymphocytes (day 28) were increased at both doses of CNT-long and CNT-COOH-low – and at highest dose of CNT-COOH-high (Supplementary materials, Table S1). On day 90, we only assessed the high dose and the only effect was that neutrophil numbers for CNT-short 54 µg were decreased as compared to control (Supplementary materials, Table S1). At 90 days post-exposure, no increases in neutrophils, lymphocytes or eosinophils were observed for any of the MWCNTs.

22

We plotted the neutrophil numbers as function of MWCNT length (Figure 6) and as function of oxidation level (Figure 7). MWCNT length correlated with neutrophil influx on day 1 (Figure 6). On day 28, CNT-long is clearly more inflammogenic than CNT-short (Figure 6). Similarly, the pristine MWCNT was more inflammogenic than the COOH-modified MWCNTs of similar length in a dose-dependent manner on day 28 (Figure 7)

Levels of DNA strand breaks

In BAL fluid cells on day 28, CNT-long increased the levels of DNA strand breaks in terms of percent DNA in the comet tail at both doses (Figure 8). CNT-COOH-high also induced DNA strand breaks, but only at the highest dose. At day 90, no effects were seen in BAL fluid cells and on day 1 only CNT-short showed an increase and only in the lowest dose (Figure 8). In lung tissue, no genotoxic effects were observed (Supplementary Figure S7); in liver only CNT-long at the lowest dose induced genotoxicity (day 1, Figure 9). There were no effects on 8-oxo-dG in lungs in any of the dose groups (data not shown). Thus, increased levels of DNA strand breaks was only observed for pristine MWCNT.

In vitro evaluation of MWCNT cyto- and genotoxicity

The cytotoxicity and genotoxicity of MWCNTs were assessed in vitro in A549 cells (Figure 10 and Supplementary Materials Figures S9 and S10). None of the MWCNTs caused loss of cell viability in the WST1 assay at the assessed dose levels. Genotoxicity was assessed at the sublethal concentration 50 µg/mL. Only CNT-COOH-high induced DNA strand breaks and/or alkali-labile sites in the alkaline version of the

23

comet assay (Figure 10). In the Fpg-modified comet assay, both pristine MWCNTs caused significantly increased DNA damage as % tail DNA, suggesting increased levels of oxidative DNA damage (Figure 10). These oxidative lesions did not lead to any DNA double-strand breaks or chromosomal damage, as assessed by 53BP1 immunostaining and in the CBMN assay, respectively. Therefore, in vitro genotoxicity was governed by oxidative events and the pristine MWCNT appeared to be most genotoxic. CNT-long and CNT-short have lower ROS production than CNT-COOH-high and CNT-COOH-low, as measured by DCF in a cell-free environment. However, ROS generation of the two COOH-modified CNTs were substantially lower than for the positive control, carbon black (Supplementary materials Figure S8).

Discussion

In the current work, we compared the safe-by-design strategies of decreasing MWCNT length and of introducing COOH-groups into the MWCNT structure. We have previously identified diameter and specific surface area as important predictors of MWCNT toxicity (Knudsen et al., 2018; Poulsen et al., 2017, 2016, 2015a, 2015b). We therefore took the approach to eliminate the effect of diameter and specific surface area by studying MWCNT with similar diameter and specific surface area, essentially only varying in MWCNT length or surface oxidation. To this end, we synthesised and characterised new MWCNTs. The MWCNTs were synthesised in a cleanroom, and subsequently stored at -20 ℃, and therefore, we regard endotoxin contamination as unlikely, but this was not confirmed experimentally. The MWCNTs contained some metal impurities. The iron content (2.9%), originating from the catalyst used in the MWCNT synthesis, was similar in all batches. The titanium content was substantial in the CNT-long and CNT-short batches, originating from the probe used during sonication to disperse and shorten the MWCNTs. However, this impurity was removed by centrifugation of both batches (the Supplemental Materials). Thus, the iron and titanium content was not different among the three batches dosed to the animals. MWCNT surface oxidation was performed using acid treatment, and XPF analysis confirmed both higher levels of C=O bonds in the surface oxidised MWCNTs, and that the majority of the C atoms were in sp^2 conformation, showing the MWCNT lattice is still intact. However, it is possible the acid treatment has induced low levels of structural imperfections, which may be the reason for the slightly increased ROS formation potential of the two surface-oxidised MWCNTs (Landry et al., 2016; Sui et al., 2009). SEM and TEM pictures of the MWCNTs (Supplementary Materials Figure S1 supplement 1) show that the dispersion of the MWCNTs was highly effective, and

25

that produced MWCNTs were present as single, fairly straight MWCNTs, even before

dispersion in the exposure vehicles (for the in vivo and in vitro studies). We used

different dispersion protocols for the in vivo and the in vitro studies. However, both

dispersion protocols involved sonication and the effect (duration times energy) was

similar for the two protocols. Moreover, the total sonication time (4 or 16 min) was very

short compared to the 10 and 70 h of sonication that were used for MWCNT shortening,

and therefore, we do not expect the dispersion protocols to affect MWCNT length.

  We assessed genotoxicity and pulmonary inflammation in vivo following

intratracheal instillation exposure. Pulmonary inflammation was assessed in terms of

increased neutrophil numbers in BAL fluid cells, as well as genotoxicity in terms of

DNA strand breaks in BAL fluid, lung and liver tissue cells. An in vitro evaluation was

done to corroborate the in vivo findings.

  Inhalation is the gold standard for risk assessment of pulmonary exposure, but

because intratracheal instillation allows full control of the dose, it is well suited for

comparison of the hazard potential of nanomaterials (Barfod et al., 2020; Bendtsen et

al., 2020, 2019; Danielsen et al., 2020; Gaté et al., 2019; Hadrup et al., 2021, 2019c,

2019b, 2019a; Saber et al., 2016, 2012, 2019; Wallin et al., 2017).

   CNT-long induced a high number of neutrophils at day 1 and day 28, and

neutrophil cell numbers were lowered at the low dose level after exposure to shorter

fibres and to surface oxidised MWCNT. This was seen both on the bar graphs (Figure 4

and 5), and when plotted as XY graphs as function of length, together with data from

(Poulsen et al., 2016), and as function of surface oxidation (Figures 6 and 7). This

suggests these safe-by-design approaches decrease MWCNT-induced inflammation.

This is in agreement with data from Poulsen *et al.* showing that MWCNTs modified

with OH or COOH exhibited lower inflammation in terms of neutrophil numbers 28

26

days after intratracheal instillation into mice (Poulsen et al., 2016). Yet looking further into our current data on other cell types in BAL fluid, there is some indication that choosing the shorter fibre strategy may be more effective than introducing COOH groups. At the day-1 time-point, macrophage numbers were decreased after CNT-long but not CNT-short, whereas the introduction of COOH groups was not different from CNT-long (Supplementary Table S1). Also looking at lymphocytes at 24 h and 28 days, it is less obvious that the introduction of COOH groups strongly lower the toxic response of CNT-long (Supplementary Table S1). It should be taken into account, that the COOH-modified MWCNTs are both slightly shorter (3.1 and 3.3 µm) than CNT-long (3.9 µm). This could contribute to the decreased toxicity. A possible mechanism underlying the decreased inflammation of the COOH-modified MWCNTs could be decreased cellular uptake. Several in vitro studies have been conducted previously. Decreased cellular uptake after coating of MWCNTs has e.g. been described with polymer coating (Ito et al., 2018) and with bovine serum albumin coating (Liu et al., 2014). By contrast, increased uptake has been demonstrated with COOH-modification of MWCNTs: THP-1 macrophages accumulated 80-100 times more MWCNT after exposure to COOH-modified MWCNT coated with Pluronic® F-108 than they accumulated a pristine counterpart. The authors of the study suggested that macrophages have selective binding sites for COOH-modified MWCNT (Wang et al., 2018). It may be important to distinguish between increased uptake by lung epithelial cells potentially leading to increased toxicity, and uptake by macrophages, whose role it is to remove foreign substances from the lung to decrease toxicity. Notably, one effect of surface coating could be different propensity to agglomerate in bodily fluids (and cell culture media) due to reduced hydrophobicity. Moreover, an altered agglomeration state may play a role in the altered uptake into cells. We did not specifically test

27

agglomeration in our in vitro cell culture medium. Notably, MWCNTs may behave differently in cell cultures, as compared to the in vivo situation - as discussed below.

For CNT-long, neutrophil influx at day 1 similar for the two dose levels. We have previously reported lack of dose response relationship for some MWCNTs even following inhalation exposure (Gaté et al., 2019; Poulsen et al., 2015b).

Concerning genotoxicity, pristine CNT-long and CNT-short induced effects in vivo. CNT-long increased genotoxicity in BAL fluid cells at both dose levels on day 28, suggesting the fibre only showed effect after prolonged exposure. In liver cells, an increased level of DNA strand breaks was seen at day 1, at the lowest dose only. For CNT-short, the effect was seen only at the lowest dose at day 1 in BAL fluid cells. We have previously reported lack of dose-response relationship for nanomaterial-induced DNA strand break levels in vivo, as determined by the comet assay (Z O Kyjovska et al., 2015; Zdenka O. Kyjovska et al., 2015), which may be caused by the low dynamic range of particle-induce DNA damage in vivo in the comet assay (Z O Kyjovska et al., 2015). The surface-oxidised MWCNT did not induce genotoxicity in vivo, suggesting that the in vivo genotoxic potential can be lowered by oxidising MWCNTs. In vitro, this was supported by the Fpg version of the comet assay in which there was no effect of the COOH-modified MWCNTs while CNT-short and CNT-long induced increased levels of Fpg-sensitive sites in the DNA. This could not be corroborated in the alkaline version of the assay, where only the CNT-COOH-high induced DNA damage (Figure 10). Perhaps the less clear in vitro results reflect that fibres may act differently in vivo (needle-like action) than in vitro (sedimentation on top of the cells). In cell free environment, CNT-long and CNT-short had lower ROS production than CNT-COOH-high and CNT-COOH-low (Supplementary materials Figure S8), suggesting that at least

28

in this endpoint adding COOH groups do not decrease the genotoxicity of MWCNTs, and that the genotoxicity of CNT-long seen in vivo is not driven by ROS production.

The notion that length is an important parameter for MWCNT toxicity, is supported by the previous literature presented in the introduction section. For instance the data from Catalan and her colleagues showed that a straight (69 x 4420 nm) MWCNT after inhalation displayed effects in the comet assay, whereas a, tangled shorter (15 x 370 nm) MWCNT did not (Catalan et al., 2016). Moreover, when rats inhaled a MWCNT 12 nm across and 0.75 µm in length no effects were observed on micronuclei formation, 8-Oxo-2'-deoxyguanosine (8-oxo-dG) levels or in the comet assay (Pothmann et al., 2015). By contrast, MWCNT-7, 5.4 to 5.9 µm in length, induced lung carcinomas in rats already at inhalation of 0.2 mg/m^3 (Kasai et al., 2016) (IARC, 2017). And a 3.1 µm long MWCNT, after trans-tracheal intrapulmonary spraying into rat lungs at 3.3 mg/kg bw (1 mg/rat), induced carcinogenicity in the form of malignant mesothelioma and lung tumours (Suzui et al., 2016). However, in these studies, both diameter and length differed between the compared MWCNTs, thus also varying the specific surface area and the rigidity of these nanomaterials. Thin MWCNTs are often entangled, whereas thick ones appear more needle-like. We have previously shown that pulmonary long-term biodistribution and histopathology differ extensively among MWCNTs of different diameter (Knudsen et al., 2018).

The current data pertains to MWCNT. A question is whether they can be extrapolated to single-walled CNT (SWCNT). Previous data on SWCNT point to different toxicokinetics. Fujita et al. compared intratracheal instillation of SWCNTs and MWCNTs in rats at doses of 0.15 and 1.5 mg/kg bw. During a 90-day post-exposure period, SWCNTs caused persistent pulmonary inflammation seen in the BAL-fluid. While short MWCNTs had a more immediate and larger impact on the alveoli that had

29

shorter duration than the SWCNT (Fujita et al., 2016). Honda et al. compared short (0.6 µm) and long (8.6 µm) SWCNTs by intratracheal instillation into rats at 0.2 and 1 mg/kg bw (long) and 1 mg/kg bw (short). Inflammatory changes and alveolar wall fibrosis were observed in the lungs after short SWCNTs, while the incidences of these changes were much lower after the longer counterpart (Honda et al., 2017).

In another comparison of short and long SWCNT, Ema et al. exposed rats by intratracheal instillation to SWCNT 0.4 or 2.8 µm long (1 mg/kg bw). The short SWCNTs caused persistent lung injury and inflammation during a 6-month observational period, while the long ones induced only minimal lung injury and inflammation (Ema et al., 2017).

These data on SWCNTs are in contrast to our data showing that longer MWCNTs have stronger effects than shorter ones. And also showing a prolonged effects of SWCNTs that we did not see at our 90 day time-point. Nonetheless, our data and those of Honda and Fujita are in line, showing that MWCNTs seem to have shorter duration of effect as compared to SWCNTs – the reason for this is unknown, but could reflect that MWCNTs are more easily removed from the lung – perhaps due to a more severe response inducing the body to eliminate the fibres.

In conclusion, we found acute and subacute inflammation to be decreased by either strategy: decreasing the length of the MWCNT or by the introduction of COOH groups. Genotoxicity was primarily reduced by surface oxidation (seen both in vivo and in vitro), while the results were less clear for MWCNT shortening The data suggests that one can employ either strategy (decreased length and oxidation) to lower, but not eliminate, the toxicity of MWCNTs.

30

CRediT author statement

Niels Hadrup: Formal analysis, Visualization, Writing- Original draft preparation.
Kristina Bram Knudsen: Conceptualization, Investigation, Writing- Reviewing and
Editing. **Marie Carriere:** Conceptualization, Investigation, Formal analysis,
Visualization, Writing- Original draft preparation. **Martine Mayne-L'Hermite:**
Conceptualization, Investigation, Formal analysis, Visualization, Writing- Original draft
preparation. **Laure Bobyk:** Investigation, Writing- Reviewing and Editing. **Soline
Allard:** Conceptualization, Investigation, Formal analysis, Visualization, Writing-
Original draft preparation. **Frédéric Miserque:** Investigation, Writing- Reviewing and
Editing. **Baptiste Pibaleau:** Investigation, Writing- Reviewing and Editing. **Mathieu
Pinault:** Investigation, Writing- Reviewing and Editing. **Håkan Wallin:**
Conceptualization, Project administration, Formal analysis, Writing- Reviewing and
Editing. **Ulla Vogel:** Conceptualization, Project administration, Formal analysis,
Writing- Original draft preparation

Declaration of interests

☒ The authors declare that they have no known competing financial interests or

personal relationships that could have appeared to influence the work reported in this

paper.

On behalf of all authors:

Niels Hadrup, Copenhagen, 4 March 2021

Acknowledgments

References

Barfod, K.K., Bendtsen, K.M., Berthing, T., Koivisto, A.J., Poulsen, S.S., Segal, E., Verleysen, E., Mast, J., Holländer, A., Jensen, K.A., Hougaard, K.S., Vogel, U., 2020. Increased surface area of halloysite nanotubes due to surface modification predicts lung inflammation and acute phase response after pulmonary exposure in mice. Environ. Toxicol. Pharmacol. 73, 103266. https://doi.org/10.1016/j.etap.2019.103266

Bendtsen, K.M., Brostrøm, A., Koivisto, A.J., Koponen, I., Berthing, T., Bertram, N., Kling, K.I., Dal Maso, M., Kangasniemi, O., Poikkimäki, M., Loeschner, K., Clausen, P.A., Wolff, H., Jensen, K.A., Saber, A.T., Vogel, U., 2019. Airport emission particles: exposure characterization and toxicity following intratracheal instillation in mice. Part. Fibre Toxicol. 16, 23. https://doi.org/10.1186/s12989-019-0305-5

Bendtsen, K.M., Gren, L., Malmborg, V.B., Shukla, P.C., Tunér, M., Essig, Y.J., Krais, A.M., Clausen, P.A., Berthing, T., Loeschner, K., Jacobsen, N.R., Wolff, H., Pagels, J., Vogel, U.B., 2020. Particle characterization and toxicity in C57BL/6 mice following instillation of five different diesel exhaust particles designed to differ in physicochemical properties. Part. Fibre Toxicol. 17, 38. https://doi.org/10.1186/s12989-020-00369-9

Brun, E., Barreau, F., Veronesi, G., Fayard, B., Sorieul, S., Chanéac, C., Carapito, C., Rabilloud, T., Mabondzo, A., Herlin-Boime, N., Carrière, M., 2014. Titanium dioxide nanoparticle impact and translocation through ex vivo, in vivo and in vitro gut epithelia. Part. Fibre Toxicol. 11, 13. https://doi.org/10.1186/1743-8977-11-13

33

Castro, C., Pinault, M., Porterat, D., Reynaud, C., Mayne-L'Hermite, M., 2013. The role of hydrogen in the aerosol-assisted chemical vapor deposition process in producing thin and densely packed vertically aligned carbon nanotubes. Carbon N. Y. 61, 585–594. https://doi.org/10.1016/j.carbon.2013.05.040

Catalan, J., Siivola, K.M., Nymark, P., Lindberg, H., Suhonen, S., Jarventaus, H., Koivisto, A.J., Moreno, C., Vanhala, E., Wolff, H., Kling, K.I., Jensen, K.A., Savolainen, K., Norppa, H., 2016. In vitro and in vivo genotoxic effects of straight versus tangled multi-walled carbon nanotubes. Nanotoxicology. 10, 794–806.

Charon, E., Pinault, M., Mayne-L'Hermite, M., Reynaud, C., 2021. One-step synthesis of highly pure and well-crystallized vertically aligned carbon nanotubes. Carbon N. Y. 173, 758–768. https://doi.org/10.1016/j.carbon.2020.10.056

Cohignac, V., Landry, M.J., Ridoux, A., Pinault, M., Annangi, B., Gerdil, A., Herlin-Boime, N., Mayne, M., Haruta, M., Codogno, P., Boczkowski, J., Pairon, J.-C., Lanone, S., 2018. Carbon nanotubes, but not spherical nanoparticles, block autophagy by a shape-related targeting of lysosomes in murine macrophages. Autophagy 14, 1323–1334. https://doi.org/10.1080/15548627.2018.1474993

Danielsen, P.H., Knudsen, K.B., Štrancar, J., Umek, P., Koklič, T., Garvas, M., Vanhala, E., Savukoski, S., Ding, Y., Madsen, A.M., Jacobsen, N.R., Weydahl, I.K., Berthing, T., Poulsen, S.S., Schmid, O., Wolff, H., Vogel, U., 2020. Effects of physicochemical properties of TiO2 nanomaterials for pulmonary inflammation, acute phase response and alveolar proteinosis in intratracheally exposed mice. Toxicol. Appl. Pharmacol. 386, 114830. https://doi.org/10.1016/j.taap.2019.114830

Ema, M., Takehara, H., Naya, M., Kataura, H., Fujita, K., Honda, K., 2017. Length effects of single-walled carbon nanotubes on pulmonary toxicity after intratracheal

instillation in rats. J. Toxicol. Sci. 42, 367–378. https://doi.org/10.2131/jts.42.367

Fenech, M., 2000. The in vitro micronucleus technique. Mutat. Res. Mol. Mech. Mutagen. 455, 81–95. https://doi.org/10.1016/S0027-5107(00)00065-8

Fujita, K., Fukuda, M., Endoh, S., Maru, J., Kato, H., Nakamura, A., Shinohara, N., Uchino, K., Honda, K., 2016. Pulmonary and pleural inflammation after intratracheal instillation of short single-walled and multi-walled carbon nanotubes. Toxicol. Lett. 257, 23–37. https://doi.org/10.1016/j.toxlet.2016.05.025

Gaté, L., Knudsen, K.B., Seidel, C., Berthing, T., Chézeau, L., Jacobsen, N.R., Valentino, S., Wallin, H., Bau, S., Wolff, H., Sébillaud, S., Lorcin, M., Grossmann, S., Viton, S., Nunge, H., Darne, C., Vogel, U., Cosnier, F., 2019. Pulmonary toxicity of two different multi-walled carbon nanotubes in rat: Comparison between intratracheal instillation and inhalation exposure. Toxicol. Appl. Pharmacol. 375, 17–31. https://doi.org/10.1016/j.taap.2019.05.001

Grosse, Y., Loomis, D., Guyton, K.Z., Lauby-Secretan, B., El Ghissassi, F., Bouvard, V., Benbrahim-Tallaa, L., Guha, N., Scoccianti, C., Mattock, H., Straif, K., International Agency for Research on Cancer Monograph Working Group, 2014. Carcinogenicity of fluoro-edenite, silicon carbide fibres and whiskers, and carbon nanotubes. Lancet. Oncol. 15, 1427–1428. https://doi.org/10.1016/S1470-2045(14)71109-X

Hadrup, N., Aimonen, K., Ilves, M., Lindberg, H., Atluri, R., Sahlgren, N.M., Jacobsen, N.R., Barfod, K.K., Berthing, T., Lawlor, A., Norppa, H., Wolff, H., Jensen, K.A., Hougaard, K.S., Alenius, H., Catalan, J., Vogel, U., 2021. Pulmonary toxicity of synthetic amorphous silica - effects of porosity and copper oxide doping. Nanotoxicology 15, 96–113. https://doi.org/10.1080/17435390.2020.1842932

Hadrup, N., Bengtson, S., Jacobsen, N.R., Jackson, P., Nocun, M., Saber, A.T., Jensen,

K.A., Wallin, H., Vogel, U., 2017. Influence of dispersion medium on

nanomaterial-induced pulmonary inflammation and DNA strand breaks:

Investigation of carbon black, carbon nanotubes and three titanium dioxide

nanoparticles. Mutagenesis 32. https://doi.org/10.1093/mutage/gex042

Hadrup, N., Knudsen, K.B., Berthing, T., Wolff, H., Bengtson, S., Kofoed, C.,

Espersen, R., Højgaard, C., Winther, J.R., Willemoës, M., Wedin, I., Nuopponen,

M., Alenius, H., Norppa, H., Wallin, H., Vogel, U., 2019a. Pulmonary effects of

nanofibrillated celluloses in mice suggest that carboxylation lowers the

inflammatory and acute phase responses. Environ. Toxicol. Pharmacol. 66, 116–

125. https://doi.org/10.1016/j.etap.2019.01.003

Hadrup, N., Rahmani, F., Jacobsen, N.R., Saber, A.T., Jackson, P., Bengtson, S.,

Williams, A., Wallin, H., Halappanavar, S., Vogel, U., 2019b. Acute phase

response and inflammation following pulmonary exposure to low doses of zinc

oxide nanoparticles in mice. Nanotoxicology 13, 1275–1292.

https://doi.org/10.1080/17435390.2019.1654004

Hadrup, N., Saber, A.T., Kyjovska, Z.O., Jacobsen, N.R., Vippola, M., Sarlin, E., Ding,

Y., Schmid, O., Wallin, H., Jensen, K.A., Vogel, U., 2019c. Pulmonary toxicity of

Fe2O3, ZnFe2O4, NiFe2O4 and NiZnFe4O8 nanomaterials: Inflammation and

DNA strand breaks. Environ. Toxicol. Pharmacol. 74, 103303.

https://doi.org/10.1016/j.etap.2019.103303

Halappanavar, S., Rahman, L., Nikota, J., Poulsen, S.S., Ding, Y., Jackson, P., Wallin,

H., Schmid, O., Vogel, U., Williams, A., 2019. Ranking of nanomaterial potency

to induce pathway perturbations associated with lung responses. NanoImpact 14,

100158. https://doi.org/10.1016/j.impact.2019.100158

Hamilton, R.F., Wu, Z., Mitra, S., Shaw, P.K., Holian, A., 2013. Effect of MWCNT

size, carboxylation, and purification on in vitro and in vivo toxicity, inflammation and lung pathology. Part. Fibre Toxicol. 10, 57. https://doi.org/10.1186/1743-8977-10-57

Heresanu, V., Castro, C., Cambedouzou, J., Pinault, M., Stephan, O., Reynaud, C., Mayne-L'Hermite, M., Launois, P., 2008. Nature of the Catalyst Particles in CCVD Synthesis of Multiwalled Carbon Nanotubes Revealed by the Cooling Step Study. J. Phys. Chem. C 112, 7371–7378. https://doi.org/10.1021/jp709825y

Honda, K., Naya, M., Takehara, H., Kataura, H., Fujita, K., Ema, M., 2017. A 104-week pulmonary toxicity assessment of long and short single-wall carbon nanotubes after a single intratracheal instillation in rats. Inhal. Toxicol. 29, 471–482. https://doi.org/10.1080/08958378.2017.1394930

IARC, 2017. IARC MONOGRAPHS ON THE EVALUATION OF CARCINOGENIC RISKS TO HUMANS: SOME NANOMATERIALS AND SOME FIBRES, VOLUME 111.

Ito, F., Hisashi, H., Toyokuni, S., 2018. Polymer coating on carbon nanotubes into Durobeads is a novel strategy for human environmental safety. Nagoya J. Med. Sci. 80, 597–604. https://doi.org/10.18999/nagjms.80.4.597

Jackson, P., Kling, K., Jensen, K.A., Clausen, P.A., Madsen, A.M., Wallin, H., Vogel, U., 2015. Characterization of genotoxic response to 15 multiwalled carbon nanotubes with variable physicochemical properties including surface functionalizations in the FE1-Muta(TM) mouse lung epithelial cell line. Environ.Mol.Mutagen. 56, 183–203.

Jackson, P., Lund, S.P., Kristiansen, G., Andersen, O., Vogel, U., Wallin, H., Hougaard, K.S., 2011. An experimental protocol for maternal pulmonary exposure in developmental toxicology. Basic Clin.Pharmacol.Toxicol. 108, 202–207.

37

Jackson, P., Pedersen, L.M., Kyjovska, Z.O., Jacobsen, N.R., Saber, A.T., Hougaard, K.S., Vogel, U., Wallin, H., 2013. Validation of freezing tissues and cells for analysis of DNA strand break levels by comet assay. Mutagenesis 28, 699–707. https://doi.org/10.1093/mutage/get049

Jacobsen, N.R., Pojana, G., White, P., Møller, P., Cohn, C.A., Smith Korsholm, K., Vogel, U., Marcomini, A., Loft, S., Wallin, H., 2008. Genotoxicity, cytotoxicity, and reactive oxygen species induced by single- walled carbon nanotubes and C 60 fullerenes in the FE1- Muta^{TM}Mouse lung epithelial cells. Environ. Mol. Mutagen. 49, 476–487. https://doi.org/10.1002/em.20406

Jagiello, K., Halappanavar, S., Rybińska-Fryca, A., Willliams, A., Vogel, U., Puzyn, T., 2021. Transcriptomics-Based and AOP-Informed Structure-Activity Relationships to Predict Pulmonary Pathology Induced by Multiwalled Carbon Nanotubes. Small 17, e2003465. https://doi.org/10.1002/smll.202003465

Kasai, T., Umeda, Y., Ohnishi, M., Mine, T., Kondo, H., Takeuchi, T., Matsumoto, M., Fukushima, S., 2016. Lung carcinogenicity of inhaled multi-walled carbon nanotube in rats. Part Fibre.Toxicol. 13, 53.

Knudsen, K.B., Berthing, T., Jackson, P., Poulsen, S.S., Mortensen, A., Jacobsen, N.R., Skaug, V., Szarek, J., Hougaard, K.S., Wolff, H., Wallin, H., Vogel, U., 2018. Physicochemical predictors of Multi-Walled Carbon Nanotube-induced pulmonary histopathology and toxicity one year after pulmonary deposition of 11 different Multi-Walled Carbon Nanotubes in mice. Basic Clin. Pharmacol. Toxicol. 124, 211–227. https://doi.org/10.1111/bcpt.13119

Kyjovska, Z O, Jacobsen, N.R., Saber, A.T., Bengtson, S., Jackson, P., Wallin, H., Vogel, U., 2015. DNA damage following pulmonary exposure by instillation to low doses of carbon black (Printex 90) nanoparticles in mice.

38

Environ.Mol.Mutagen. 56, 41–49.

Kyjovska, Zdenka O., Jacobsen, N.R., Saber, A.T., Bengtson, S., Jackson, P., Wallin, H., Vogel, U., 2015. DNA strand breaks, acute phase response and inflammation following pulmonary exposure by instillation to the diesel exhaust particle NIST1650b in mice. Mutagenesis 30, 499–507. https://doi.org/10.1093/mutage/gev009

Landry, M., Pinault, M., Tchankouo, S., Charon, É., Ridoux, A., Boczkowski, J., Mayne-L'Hermite, M., Lanone, S., 2016. Early signs of multi-walled carbon nanotbues degradation in macrophages, via an intracellular pH-dependent biological mechanism; importance of length and functionalization. Part. Fibre Toxicol. 13, 61. https://doi.org/10.1186/s12989-016-0175-z

LeBel, C.P., Ischiropoulos, H., Bondy, S.C., 1992. Evaluation of the probe 2',7'-dichlorofluorescin as an indicator of reactive oxygen species formation and oxidative stress. Chem. Res. Toxicol. 5, 227–231. https://doi.org/10.1021/tx00026a012

Liu, Y., Ren, L., Yan, D., Zhong, W., 2014. Mechanistic Study on the Reduction of SWCNT-induced Cytotoxicity by Albumin Coating. Part. Part. Syst. Charact. Meas. Descr. Part. Prop. Behav. powders other disperse Syst. 31, 1244–1251. https://doi.org/10.1002/ppsc.201400145

Maultzsch, J., Reich, S., Thomsen, C., Webster, S., Czerw, R., Carroll, D.L., Vieira, S.M.C., Birkett, P.R., Rego, C.A., 2002. Raman characterization of boron-doped multiwalled carbon nanotubes. Appl. Phys. Lett. 81, 2647–2649. https://doi.org/10.1063/1.1512330

Muller, J., Delos, M., Panin, N., Rabolli, V., Huaux, F., Lison, D., 2009. Absence of carcinogenic response to multiwall carbon nanotubes in a 2-year bioassay in the

39

peritoneal cavity of the rat. Toxicol.Sci. 110, 442–448.

Nagai, H., Okazaki, Y., Chew, S.H., Misawa, N., Yamashita, Y., Akatsuka, S., Ishihara, T., Yamashita, K., Yoshikawa, Y., Yasui, H., Jiang, L., Ohara, H., Takahashi, T., Ichihara, G., Kostarelos, K., Miyata, Y., Shinohara, H., Toyokuni, S., 2011. Diameter and rigidity of multiwalled carbon nanotubes are critical factors in mesothelial injury and carcinogenesis. Proc. Natl. Acad. Sci. U. S. A. 108, E1330-8. https://doi.org/10.1073/pnas.1110013108

Pimenta, M.A., Dresselhaus, G., Dresselhaus, M.S., Cançado, L.G., Jorio, A., Saito, R., 2007. Studying disorder in graphite-based systems by Raman spectroscopy. Phys. Chem. Chem. Phys. 9, 1276–1290. https://doi.org/10.1039/B613962K

Pothmann, D., Simar, S., Schuler, D., Dony, E., Gaering, S., Le Net, J.L., Okazaki, Y., Chabagno, J.M., Bessibes, C., Beausoleil, J., Nesslany, F., Regnier, J.F., 2015. Lung inflammation and lack of genotoxicity in the comet and micronucleus assays of industrial multiwalled carbon nanotubes Graphistrength((c)) C100 after a 90-day nose-only inhalation exposure of rats. Part Fibre.Toxicol. 12, 21.

Poulsen, S., Jacobsen, N.R., Labib, S., Wu, D., Husain, M., Williams, A., Bogelund, J.P., Andersen, O., Kobler, C., Molhave, K., Kyjovska, Z.O., Saber, A.T., Wallin, H., Yauk, C.L., Vogel, U., Halappanavar, S., 2013. Transcriptomic analysis reveals novel mechanistic insight into murine biological responses to multi-walled carbon nanotubes in lungs and cultured lung epithelial cells. PLoS.One. 8, e80452.

Poulsen, S.S., Jackson, P., Kling, K., Knudsen, K.B., Skaug, V., Kyjovska, Z.O., Thomsen, B.L., Clausen, P.A., Atluri, R., Berthing, T., Bengtson, S., Wolff, H., Jensen, K.A., Wallin, H., Vogel, U., 2016. Multi-walled carbon nanotube physicochemical properties predict pulmonary inflammation and genotoxicity. Nanotoxicology. 10, 1263–1275.

Poulsen, S.S., Knudsen, K.B., Jackson, P., Weydahl, I.E.K., Saber, A.T., Wallin, H., Vogel, U., 2017. Multi-walled carbon nanotube-physicochemical properties predict the systemic acute phase response following pulmonary exposure in mice. PLoS One 12, e0174167. https://doi.org/10.1371/journal.pone.0174167

Poulsen, S.S., Saber, A.T., Mortensen, A., Szarek, J., Wu, D., Williams, A., Andersen, O., Jacobsen, N.R., Yauk, C.L., Wallin, H., Halappanavar, S., Vogel, U., 2015a. Changes in cholesterol homeostasis and acute phase response link pulmonary exposure to multi-walled carbon nanotubes to risk of cardiovascular disease. Toxicol.Appl.Pharmacol. 283, 210–222.

Poulsen, S.S., Saber, A.T., Williams, A., Andersen, O., Kobler, C., Atluri, R., Pozzebon, M.E., Mucelli, S.P., Simion, M., Rickerby, D., Mortensen, A., Jackson, P., Kyjovska, Z.O., Molhave, K., Jacobsen, N.R., Jensen, K.A., Yauk, C.L., Wallin, H., Halappanavar, S., Vogel, U., 2015b. MWCNTs of different physicochemical properties cause similar inflammatory responses, but differences in transcriptional and histological markers of fibrosis in mouse lungs. Toxicol.Appl.Pharmacol. 284, 16–32.

Ravanat, J.-L., 2002. Cellular background level of 8-oxo-7,8-dihydro-2'-deoxyguanosine: an isotope based method to evaluate artefactual oxidation of DNA during its extraction and subsequent work-up. Carcinogenesis 23, 1911–1918. https://doi.org/10.1093/carcin/23.11.1911

Rittinghausen, S., Hackbarth, A., Creutzenberg, O., Ernst, H., Heinrich, U., Leonhardt, A., Schaudien, D., 2014. The carcinogenic effect of various multi-walled carbon nanotubes (MWCNTs) after intraperitoneal injection in rats. Part. Fibre Toxicol. 11, 59. https://doi.org/10.1186/s12989-014-0059-z

Rota, C., Chignell, C.F., Mason, R.P., 1999. Evidence for free radical formation during

the oxidation of 2′-7′-dichlorofluorescin to the fluorescent dye 2′-7′-dichlorofluorescein by horseradish peroxidase:Possible implications for oxidative stress measurements. Free Radic. Biol. Med. 27, 873–881. https://doi.org/10.1016/S0891-5849(99)00137-9

Rothkamm, K., Barnard, S., Moquet, J., Ellender, M., Rana, Z., Burdak-Rothkamm, S., 2015. DNA damage foci: Meaning and significance. Environ. Mol. Mutagen. 56, 491–504. https://doi.org/10.1002/em.21944

Saber, A.T., Jacobsen, N.R., Mortensen, A., Szarek, J., Jackson, P., Madsen, A.M., Jensen, K.A., Koponen, I.K., Brunborg, G., Gutzkow, K.B., Vogel, U., Wallin, H., 2012. Nanotitanium dioxide toxicity in mouse lung is reduced in sanding dust from paint. Part Fibre.Toxicol. 9, 4.

Saber, A.T., Mortensen, A., Szarek, J., Jacobsen, N.R., Levin, M., Koponen, I.K., Jensen, K.A., Vogel, U., Wallin, H., 2019. Toxicity of pristine and paint-embedded TiO2 nanomaterials. Hum. Exp. Toxicol. 38, 11–24. https://doi.org/10.1177/0960327118774910

Saber, A.T., Mortensen, A., Szarek, J., Koponen, I.K., Levin, M., Jacobsen, N.R., Pozzebon, M.E., Mucelli, S.P., Rickerby, D.G., Kling, K., Atluri, R., Madsen, A.M., Jackson, P., Kyjovska, Z.O., Vogel, U., Jensen, K.A., Wallin, H., 2016. Epoxy composite dusts with and without carbon nanotubes cause similar pulmonary responses, but differences in liver histology in mice following pulmonary deposition. Part Fibre.Toxicol. 13, 37.

Saleh, D.M., Alexander, W.T., Numano, T., Ahmed, O.H.M., Gunasekaran, S., Alexander, D.B., Abdelgied, M., El-Gazzar, A.M., Takase, H., Xu, J., Naiki-Ito, A., Takahashi, S., Hirose, A., Ohnishi, M., Kanno, J., Tsuda, H., 2020. Comparative carcinogenicity study of a thick, straight-type and a thin, tangled-type

multi-walled carbon nanotube administered by intra-tracheal instillation in the rat. Part. Fibre Toxicol. 17, 48. https://doi.org/10.1186/s12989-020-00382-y

Sargent, L.M., Porter, D.W., Staska, L.M., Hubbs, A.F., Lowry, D.T., Battelli, L., Siegrist, K.J., Kashon, M.L., Mercer, R.R., Bauer, A.K., Chen, B.T., Salisbury, J.L., Frazer, D., McKinney, W., Andrew, M., Tsuruoka, S., Endo, M., Fluharty, K.L., Castranova, V., Reynolds, S.H., 2014. Promotion of lung adenocarcinoma following inhalation exposure to multi-walled carbon nanotubes. Part Fibre.Toxicol. 11, 3.

Sui, X.-M., Giordani, S., Prato, M., Wagner, H.D., 2009. Effect of carbon nanotube surface modification on dispersion and structural properties of electrospun fibers. Appl. Phys. Lett. 95, 233113. https://doi.org/10.1063/1.3272012

Suzui, M., Futakuchi, M., Fukamachi, K., Numano, T., Abdelgied, M., Takahashi, S., Ohnishi, M., Omori, T., Tsuruoka, S., Hirose, A., Kanno, J., Sakamoto, Y., Alexander, D.B., Alexander, W.T., Jiegou, X., Tsuda, H., 2016. Multiwalled carbon nanotubes intratracheally instilled into the rat lung induce development of pleural malignant mesothelioma and lung tumors. Cancer Sci. 107, 924–935.

Takagi, A., Hirose, A., Futakuchi, M., Tsuda, H., Kanno, J., 2012. Dose-dependent mesothelioma induction by intraperitoneal administration of multi-wall carbon nanotubes in p53 heterozygous mice. Cancer Sci. 103, 1440–4. https://doi.org/10.1111/j.1349-7006.2012.02318.x

Wallin, H., Kyjovska, Z.O., Poulsen, S.S., Jacobsen, N.R., Saber, A.T., Bengtson, S., Jackson, P., Vogel, U., 2017. Surface modification does not influence the genotoxic and inflammatory effects of TiO2 nanoparticles after pulmonary exposure by instillation in mice. Mutagenesis 32, 47–57.

Wang, R., Lee, M., Kinghorn, K., Hughes, T., Chuckaree, I., Lohray, R., Chow, E.,

Pantano, P., Draper, R., 2018. Quantitation of cell-associated carbon nanotubes: selective binding and accumulation of carboxylated carbon nanotubes by macrophages. Nanotoxicology 12, 677–698. https://doi.org/10.1080/17435390.2018.1472309

44

Figure Captions
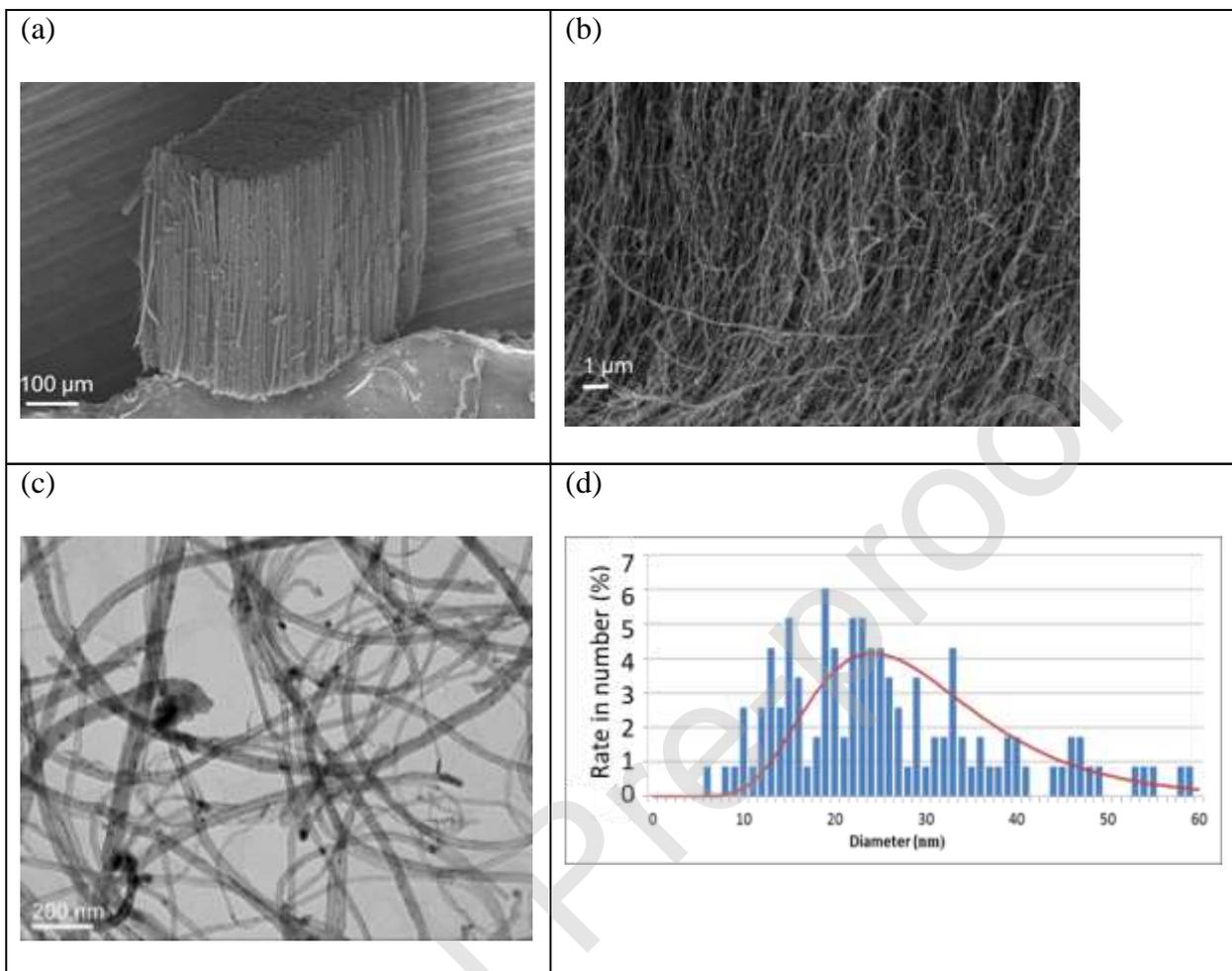
Figure 1. Electron microscopy micrographs and distribution of MWCNTs: (a) SEM micrograph of MWCNTs just after synthesis, they are vertically aligned and look like a carpet. (b) Higher magnification of raw MWCNT showing their purity (no carbonaceous by-products). (c) TEM micrograph of MWCNT after dispersion showing their morphology and diameter and confirming the absence of no carbonaceous by-products (d) MWCNT external diameter distribution measured from the TEM micrographs of the pristine MWCNT batch.

45
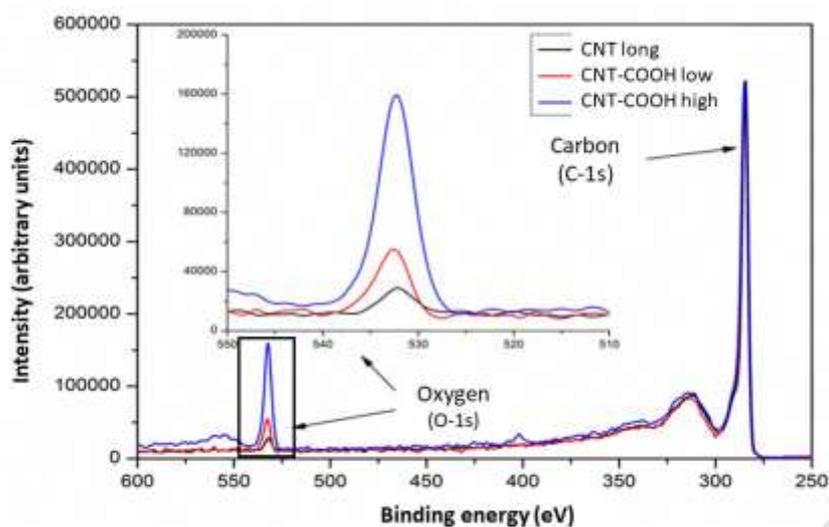
Figure 2: XPS spectra comparison of CNT-long, CNT-COOH-high and CNT-COOH-low samples. Base spectrum: survey with intensities normalised to that of C-1s peak. Top: magnification of O1s peak showing an increase of the intensity when the acid treatment duration increases.
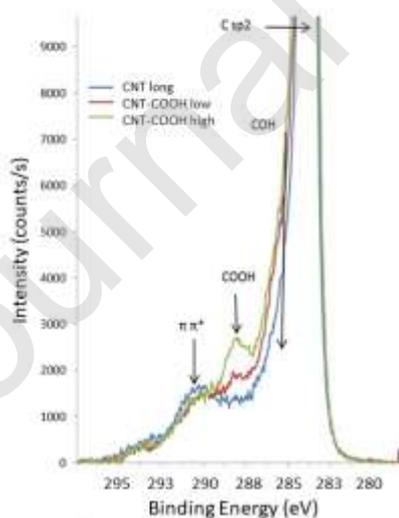
Figure 3: Normalised C-1s spectrum of CNT-COOH-high, CNT-COOH-low and raw sample. The graph shows the chemical contribution of oxygen on the C1s

46

spectrum, especially the occurrence of COOH bonds with an intensity magnification when the acid treatment duration increases.
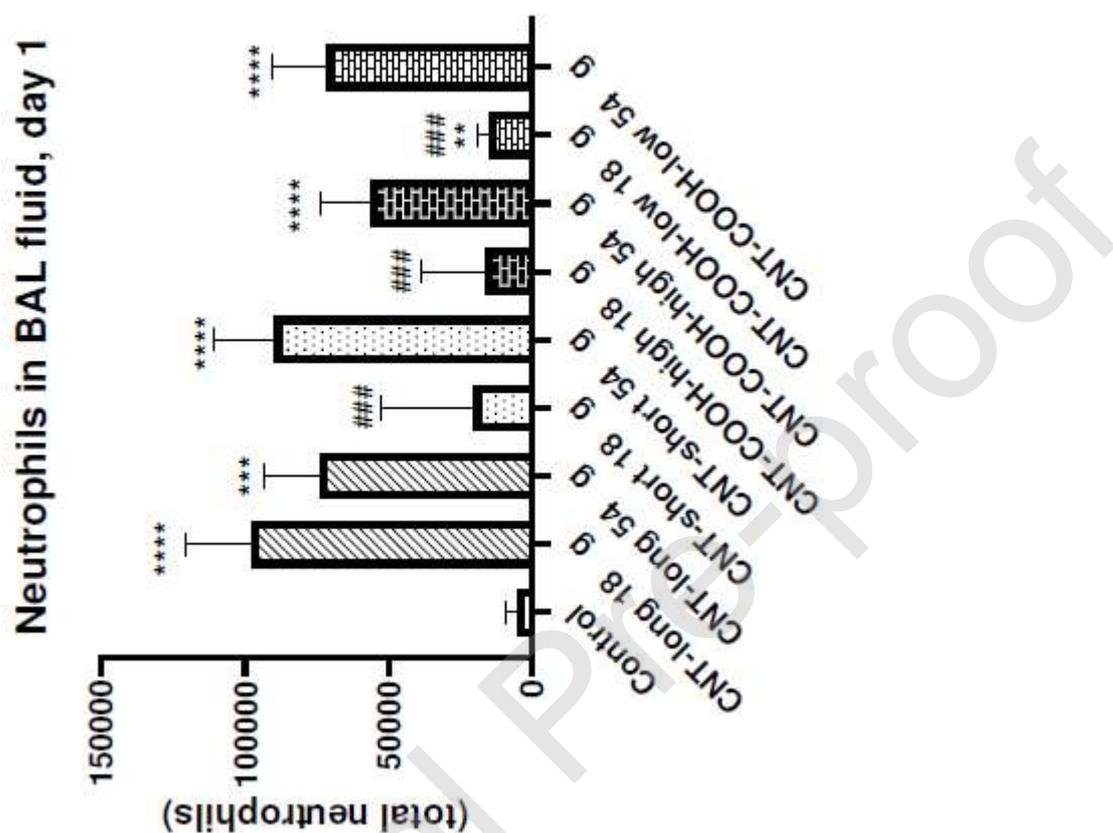

Figure 4. Neutrophils in BAL fluid at 1 day after MWCNT exposure. CNT-long, CNT-short, CNT-COOH-high or CNT-COOH-low were administered by intratracheal instillation at 18 or 54 µg/mouse. One day post-exposure, BAL fluid was recovered and the number of neutrophils determined by differential counting. Data are mean and bars represent SD. ****, ***, ** and * designates p-values of <0.0001, <0.001, <0.01 and <0.05 respectively of one way ANOVA with Holm-Sidak's multiple comparisons test compared to control in case of data approaching normality and not having a highly different variation (details given in the methods section), otherwise by Kruskall-Wallis test with Dunn's multiple comparisons test compared to control. ### designates a

Bonferroni-corrected (6 comparisons) *p*-value of <0.001 of unpaired *t*-test *vs.* each respective dose level of CNT-long.
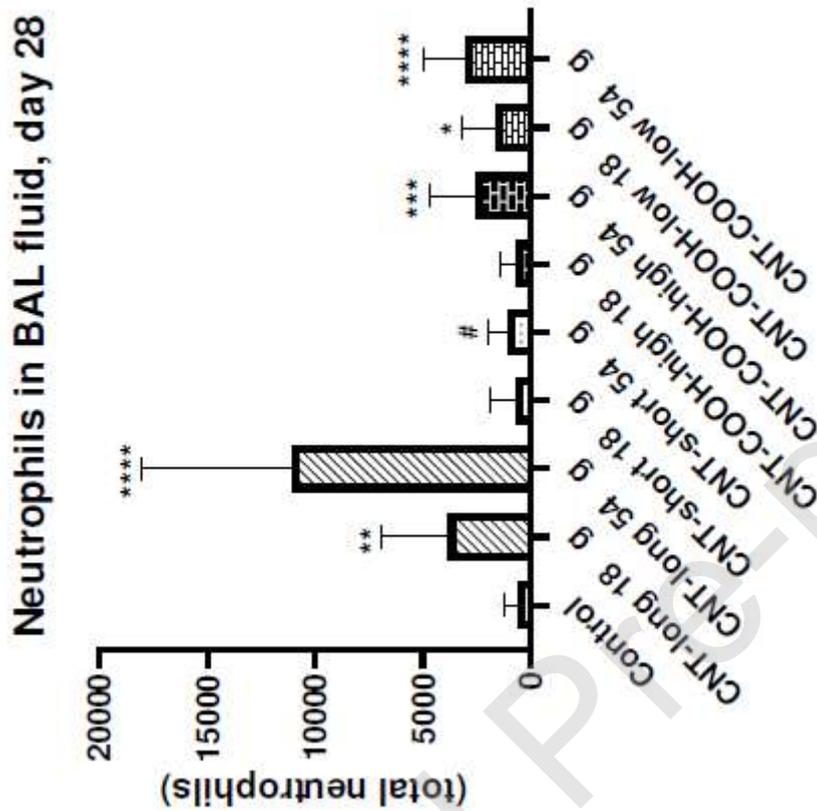
Figure 5. Neutrophils in BAL fluid at 28 days after MWCNT exposure. CNT-long, CNT-short, CNT-COOH-high or CNT-COOH-low were administered by intratracheal instillation at 18 or 54 µg/mouse. Twenty-eight days post-exposure, BAL fluid was recovered and the number of neutrophils determined by differential counting. Data are mean and bars represent SD. ****, ***, ** and * designates *p*-values of <0.0001, <0.001, <0.01 and <0.05 respectively of one way ANOVA with Holm-Sidak's multiple comparisons test compared to control in case of data approaching normality and not having a highly different variation (details given in the methods section), otherwise by Kruskall-Wallis test with Dunn's multiple comparisons test compared to control. # designates a Bonferroni-corrected (6 comparisons) *p*-value of <0.05 of unpaired *t*-test *vs.* 54 µg of CNT-long.

48
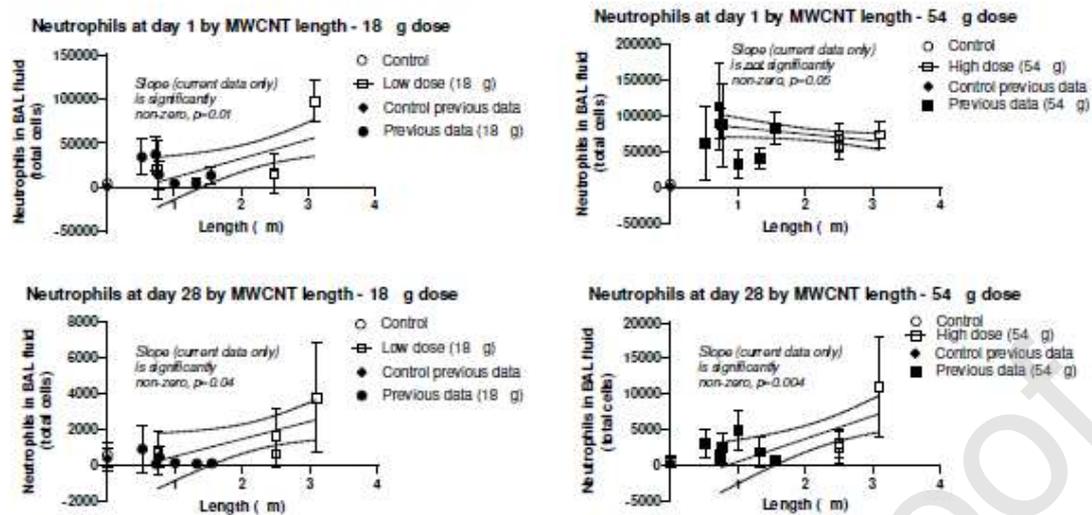
Figure 6. Neutrophil numbers in BAL fluid plotted as function of MWCNT length.
Control was set to 0 µm in length. Previous data inserted for comparison are on
MWCNTs NRCWE-040 to -045, published in (Poulsen et al., 2016). Statistical testing
was done using Linear Regression using only the data points for the MWCNTs of the
current data (control not included), *p*-values are provided in the graphs. Dotted lines
show the 95% confidence bands of the best-fit line.

49
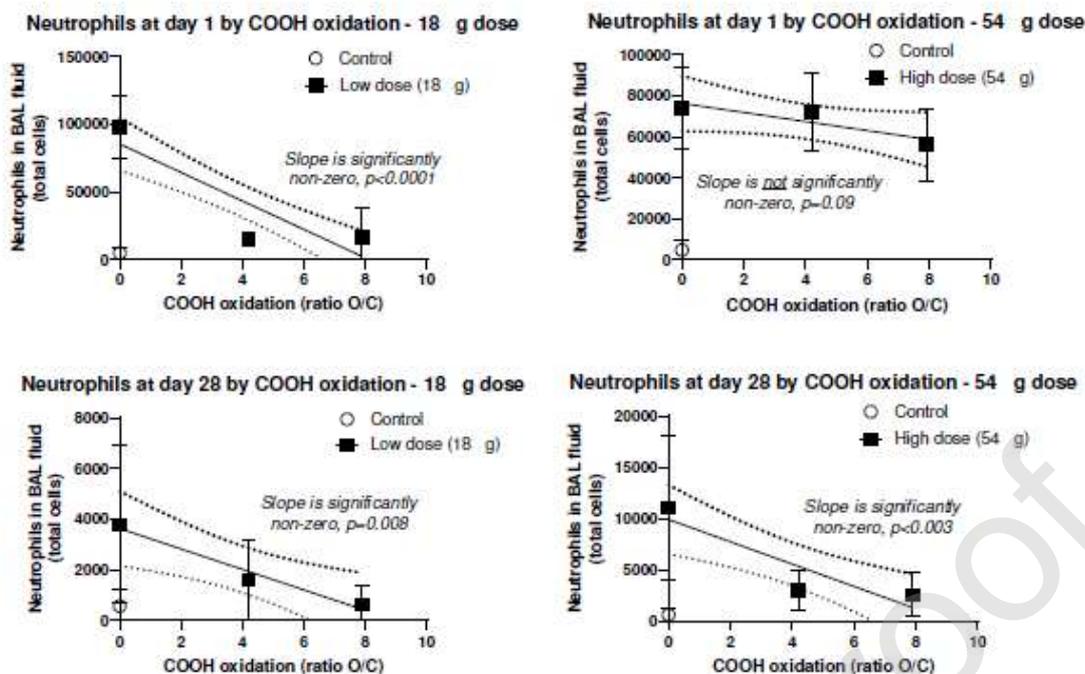
Figure 7. Neutrophil numbers in BAL fluid plotted as function of MWCNT COOH oxidation. Control as well CNT-long were set to 0 in oxidation (ratio O/C). CNT-short was omitted from the analysis in order to keep length constant. Statistical testing was done using Linear Regression using only the data points for the MWCNTs (controls not included), *p*-values are provided in the graphs. Dotted lines show the 95% confidence bands of the best-fit line.
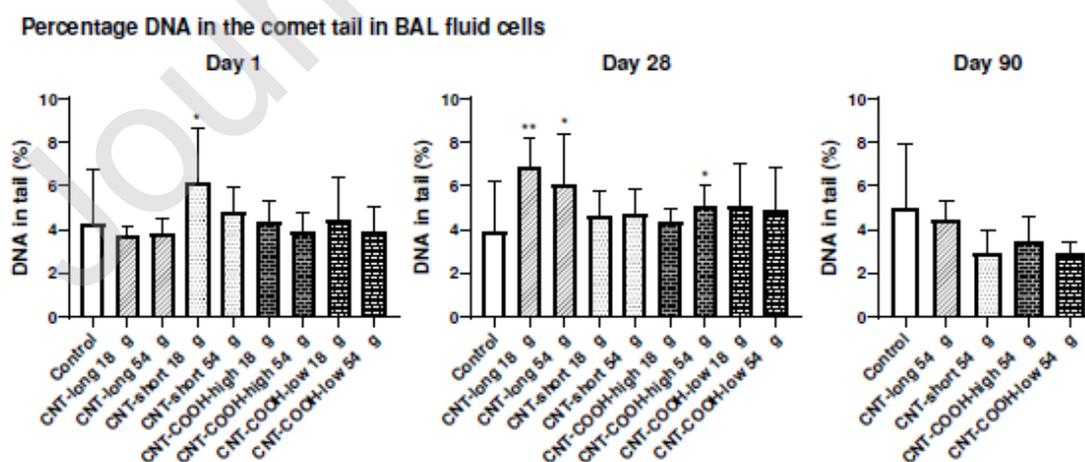
Figure 8. Levels of DNA strand breaks in BAL fluid at 1, 28 and 90 days of MWCNT exposure. CNT-long, CNT-short, CNT-COOH-high or CNT-COOH-low were administered by intratracheal instillation at 18 or 54 µg/mouse. One, 28 or 90 days post-exposure BAL fluid cells were prepared and levels of DNA strand breaks measured as percent DNA in the tail by comet assay. Data are mean and bars represent SD. ** and * designates p-values of <0.01 and <0.05 respectively of one way ANOVA with Holm-Sidak's multiple comparisons test compared to control in case of data approaching normality and not having a highly different variation (details given in the methods section), otherwise by Kruskall-Wallis test with Dunn's multiple comparisons test compared to control. The data were not tested across materials as dose-response relations are seldom seen for genotoxicity in the comet assay.


Percentage DNA in the comet tail in liver
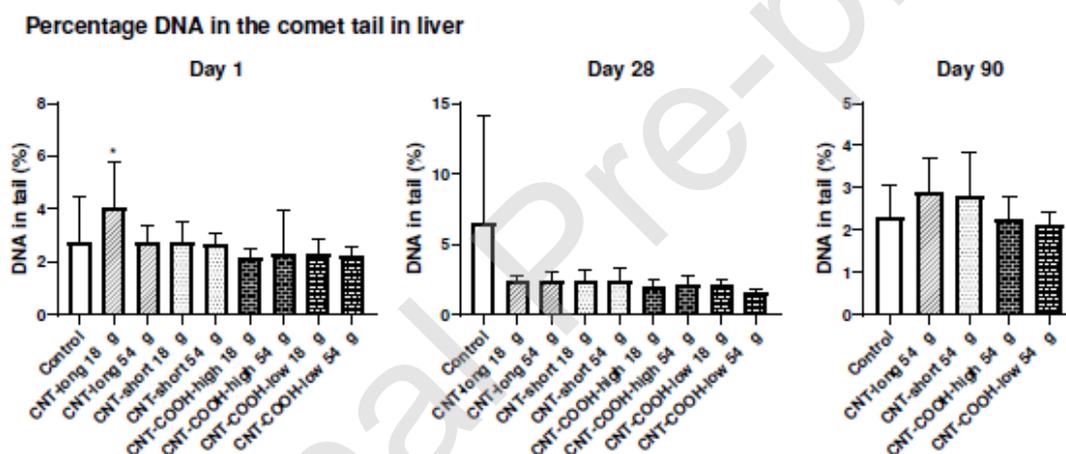
Figure 9. Levels of DNA strand breaks in liver at 1, 28 and 90 days of MWCNT exposure. CNT-long (pristine), CNT-short, CNT-COOH-high or CNT-COOH-low were administered by intratracheal instillation at 18 or 54 µg/mouse. One, 28 or 90 days post-exposure liver cells were prepared and levels of DNA strand breaks measured as percent DNA in the tail by comet assay. Data are mean and bars represent SD. * designates a p-value of <0.05 of Kruskall-Wallis test with Dunn's multiple comparisons test compared to control.
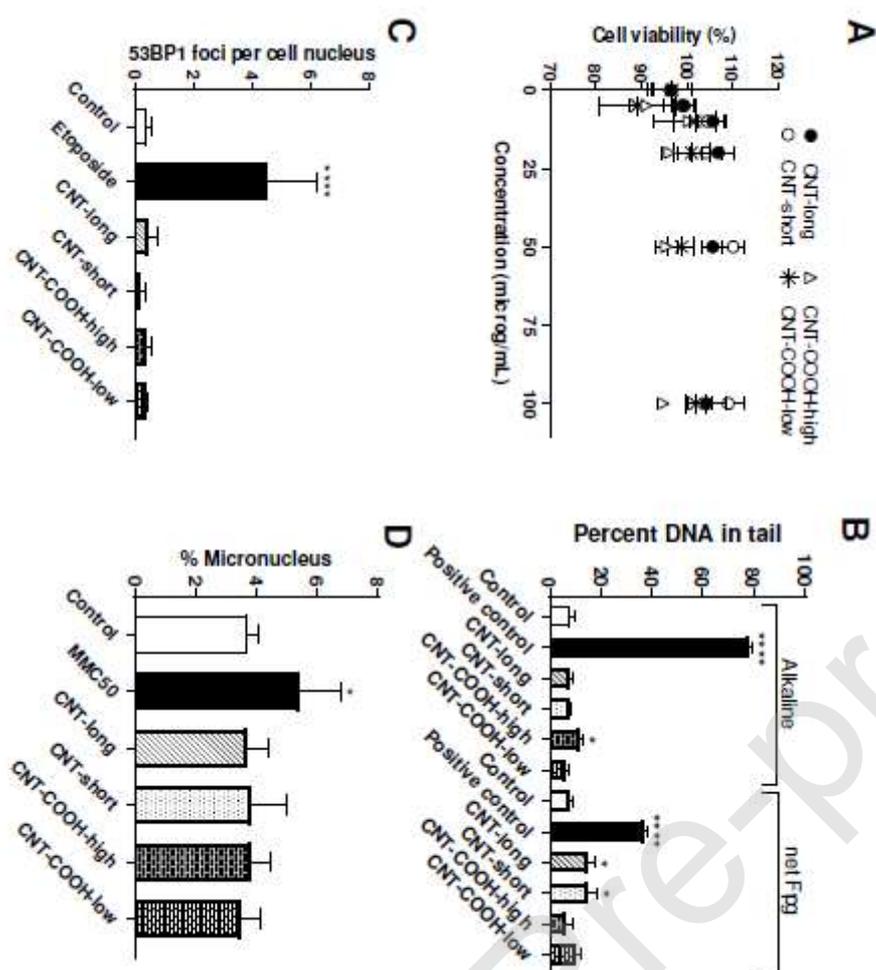
Figure 10. In vitro toxicity of MWCNTs. Cytotoxicity and genotoxicity were evaluated via WST1 assay (A), comet assay (B), 53BP1 immunostaining and foci counting (C) and cytokinesis-blocked micronucleus assay (D), in cells exposed for 24 h to 0-100 µg/mL MWCNTs (A) or to 50 µg/mL MWCNTs (B-D). Positive controls were H_2O_2 and riboflavin/UVA in the comet assay, alkaline and Fpg-modified, respectively (A); 10 µM etoposide (C) and 50 ng/mL mitomycin C (MMC50) (D). Data are mean and bars designate SD. ****, * designate p-values of <0.0001 and 0.05, exposed vs. control by Dunnett's multiple comparisons test post-test of one-way ANOVA.

52

Tables

Table 1. Physico-chemical properties of the four batches of MWCNTs.

Measurements were performed on MWCNT batches obtained after the first preparation step.

Batch	Mean length (μm) of MWCNT batches	O/C ratio (%)	Structure (Raman) ID/IG ratio
1 CNT-long	3.9 ± 2.7	0.6	0.37 ± 0.01
2 CNT-short	1.0 ± 0.6	0.6	0.39 ± 0.01
3 CNT-COOH-high	3.1 ± 1.8	7.0	0.50 ± 0.03
4 CNT-COOH-low	3.3 ± 2.4	3.6	0.35 ± 0.03

Table 2. Binding energy of the different peaks for CNT-COOH-high and -low samples.

Peak	C sp^2	C sp^3	C-OH	COOH	π-π*
Binding energy (eV)	284.1 ± 0.3	285.8 ± 0.3	286.7 ± 0.3	288.8 ± 0.3	291.5 ± 0.3

53